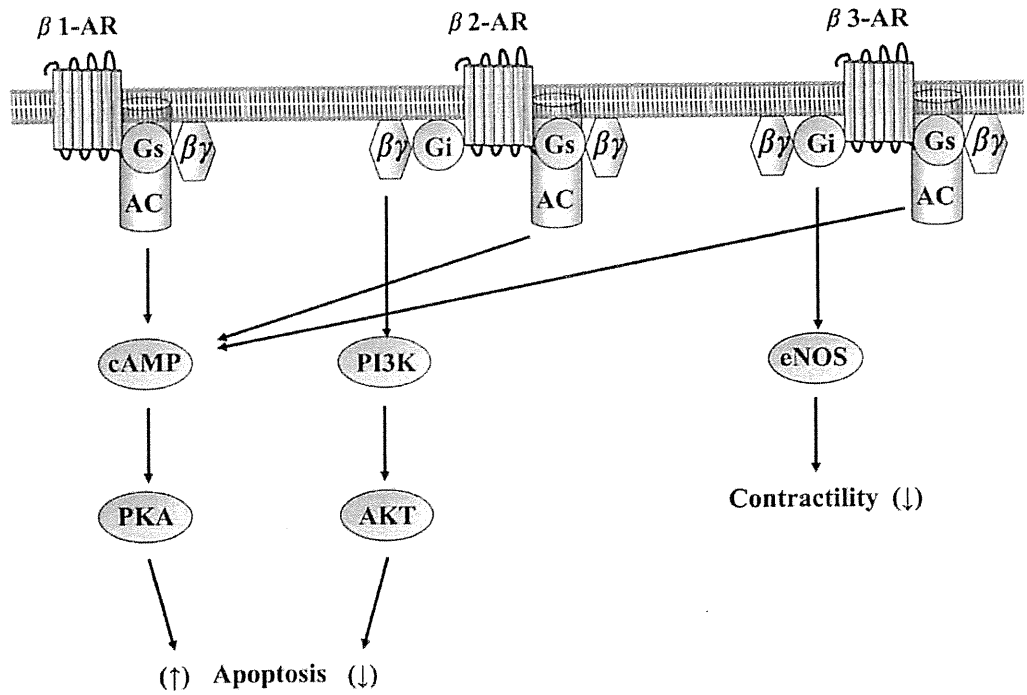

Figure 1. The β-adrenergic receptor (β-AR) receptor-mediated signaling pathway for apoptosis. Three β-AR subtypes (β1-AR, β2-AR, and β3-AR) are expressed in cardiomyocytes. Although all 3 subtypes are coupled to Gs, β2-AR and β3-AR are also linked to the Gi protein. β1-AR is thought to be mainly involved in the apoptosis of cardiomyocytes. β2-AR exerts antiapoptotic effects through Giβγ, PI3K, and AKT activation. β3-AR negatively modulates ventricular contractility through endothelial nitric oxide synthase (eNOS) activation.

cyclase (AC) and cyclic adenosine monophosphate (cAMP).[2] PKA-mediated phosphorylation of many calcium-handling molecules enhances ventricular wall motion.[13] However, long-term stimulation of these receptors can lead to the deterioration of cardiac function. In addition, the prognosis of HF patients improves with β-AR blocking therapy.[14] One of the mechanisms that contributes to this phenomenon is thought to be the induction of apoptosis upon β-AR stimulation.[15] Failing hearts have been shown to have desensitized β-adrenergic receptor signaling. This response may help maintain cardiac function.[16]

Three β-AR subtypes (β1-AR, β2-AR, and β3-AR) are expressed in cardiomyocytes (**Figure 1**). Norepinephrine or isoproterenol stimulates all β-AR subtypes and induces apoptosis in rat cardiomyocytes. However, not all subtypes of β-AR-mediated signaling induce cardiomyocyte apoptosis. It is thought that the β1-AR-mediated pathway mainly contributes to apoptosis.[17] Although all 3 subtypes are coupled to Gs, β2-AR and β3-AR are also linked to the Gi protein. The β2-AR exerts antiapoptotic effects through Giβγ, phosphatidyl inositol-3 kinase (PI3K), and AKT activation.[18] In a rat model of myocardial infarction, treating with β2-AR agonists for 2 weeks preserved cardiac contractility and reduced the number of apoptotic cardiomyocytes.[19] The β3-AR expression is upregulated in the failing heart.[20] It is reported that β3-AR negatively modulates ventricular contractility by activating endothelial nitric oxide synthase.[21] Although the role of β3-AR-mediated signaling in cardiomyocyte apoptosis is still unknown, it is possible that β3-AR exerts antiapoptotic effects through nitric oxide.[22]

Several mechanisms of β-AR stimulation-induced apoptosis have been reported.

Inducible cAMP Early Repressor (ICER)

ICERs are a group of proteins that are produced from the cAMP responsive element modulator (CREM) gene and known to induce apoptosis. PKA, which is activated by β-AR stimulation, is a key molecule that maintains ICER expression. PKA activates the cAMP-responsive element binding protein (CREB), which transactivates ICER. In addition, PKA stabilizes ICER by reducing ubiquitination.[23] Moreover, ICER attenuates phosphodiesterase (PDE) 3A transcription by interacting with the promoter region of the PDE3A gene. The downregulation of PDE3A results in elevated cAMP levels. Consequently, cAMP–PKA–ICER–PDE forms a positive feedback loop that maintains ICER expression.

ICER promotes apoptosis by downregulating Bcl-2, which is an antiapoptotic protein. Consistent with this function, isoproterenol-treated cardiomyocytes were shown to have induced ICER expression, enhanced apoptosis, and decreased Bcl-2 expression.[24] In addition, similar results were obtained in cardiomyocytes that overexpressed ICER.

ICER includes a DNA-binding domain for a cAMP-responsive element (CRE), but lacks the CREM transactivation domain. Therefore, ICER inhibits CRE-mediated transcription by CREM/CREB. Inhibiting CRE-mediated transactiva-

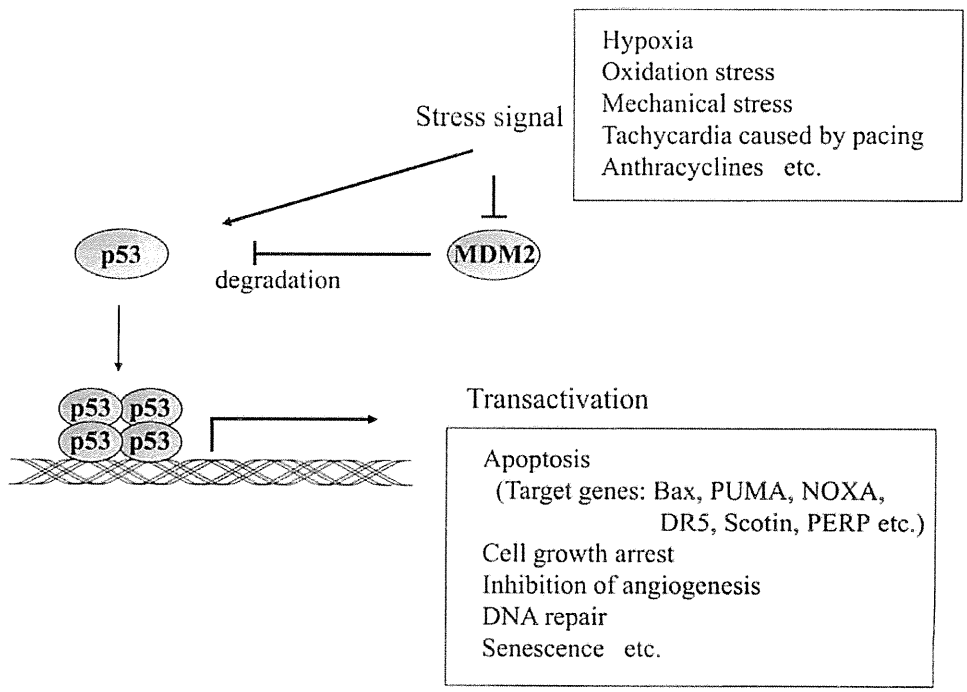

Figure 2. p53-mediated signaling pathway for apoptosis. Stresses that cause heart failure, including hypoxia, tachycardia caused by pacing, oxidative stress, mechanical stress, and anthracyclines, induce the accumulation of p53. The p53 expression level is regulated by MDM2 and MDM4, which promote the ubiquitination and degradation of p53. Accumulated p53 forms tetramers and activates the transcription of various molecules that induce apoptosis and cell growth arrest and inhibit angiogenesis, DNA repair, senescence, etc.

tion of antiapoptotic signaling is thought to be another mechanism of ICER-induced apoptosis.

Ca^{2+}/Calmodulin Kinase (CaMK), Calcineurin

β-AR stimulation increases intracellular Ca^{2+} through the L-type Ca^{2+} channel, which is essential for the proapoptotic effects of β-adrenergic stimuli. The elevated intracellular Ca^{2+} levels induce the activation of Ca^{2+}-dependent kinase, CaMK, and the phosphatase, calcineurin. Both of these proteins reportedly mediate β-adrenergic signaling-induced apoptosis. The increase in the intracellular Ca^{2+} concentration and CaMK activity is induced in a PKA-independent manner in cardiomyocytes.[25] However, the detailed mechanisms that lead to the proapoptotic effects of these proteins remain controversial. Calcineurin-independent induction of apoptosis was also observed in isoproterenol-treated cardiomyocytes.[26,27]

Exchange Protein Directly Activated by cAMP (EPAC)

cAMP, which can be induced by β-AR stimulation, activates EPAC independently of PKA.[28] EPAC, a guanine nucleotide exchange factor for the Ras-like GTPase, is involved in several cellular processes, including cell differentiation, cell proliferation, cell survival, etc. EPAC was shown to exert proapoptotic effects by inducing Bim in neuronal cells.[11] Bim directly binds to the antiapoptotic protein Bcl-2, thereby inhibiting its function.[29] However, EPAC may not play a central role in cardiomyocyte apoptosis. Overexpressing EPAC in cardiomyocytes does not induce significant apoptosis and 1 reason for this finding may be that the heart does not express Bim.

p53-Mediated Apoptosis of Cardiomyocytes

p53 is one of the most famous proteins and a major tumor suppressor, which is a group of proteins that have been well studied in cancer research.[30] Mutations in the p53 gene that attenuate p53 function have been found in 50% of human cancers.[31] This finding indicates the importance of p53 in preventing cancer. p53 mainly functions as a transcription factor and induces a variety of molecules that induce apoptosis (Bax, p53 upregulated modulator of apoptosis (PUMA), NOXA, Death receptor 5 (DR5), Scotin, p53 apoptosis effector related to PMP-22 (PERP) etc.), arrest cell growth, inhibit angiogenesis, function in DNA repair, regulate senescence, etc (Figure 2). Accumulating evidence has elucidated the importance of p53 in various cellular responses. p53 is recognized as a key molecule in the adaptation to a wide variety of harmful stimuli, including hypoxia, oxidative stress, infection, etc. In the cardiovascular system, p53 was recently shown to have a crucial function in the development of HF, arteriosclerosis, cell senescence, metabolism, etc.

We review those reports on the relationship between p53 and HF with particular emphasis on the apoptosis of cardiomyocytes.

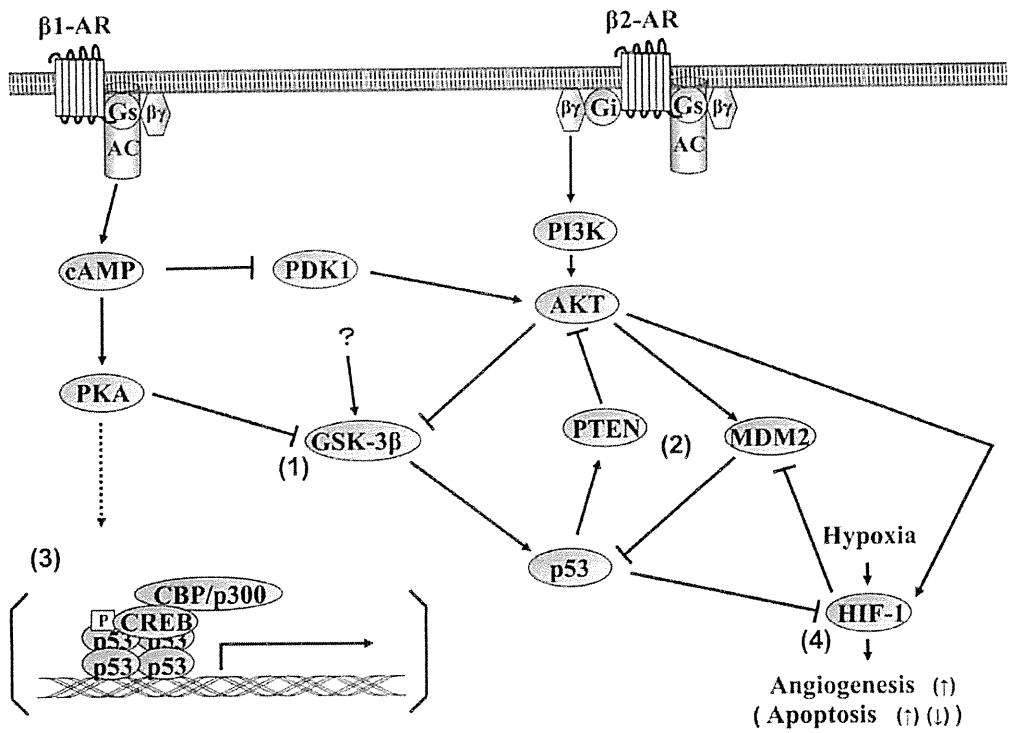

Figure 3. Cross-talk between the β-adrenergic receptor (β-AR)–mediated proapoptotic signaling pathway and p53-mediated signaling pathways. (1) Glycogen synthase kinase (GSK)-3β, (2) phosphatase and tensin homolog (PTEN)–AKT–MDM2–p53 loop, (3) cyclic adenosine monophosphate response element-binding protein (CBP)/p300–cyclic adenosine monophosphate-responsive element binding protein (CREB)–p53 complex, (4) hypoxia-inducible factor-1 (HIF-1).

p53 Expression During Stresses That Cause HF

A number of reports indicate that p53 expression is upregulated in the heart by the stresses that cause HF. Specifically, reports have shown that p53 is upregulated in the heart by ischemia,[32,33] oxidative stress,[34] mechanical stress,[35] and tachycardia caused by pacing.[36] Anthracyclines are anticancer agents that have been shown to cause cardiomyopathy, which leads to HF. Many reports demonstrated that treating with anthracyclines also induces p53 expression in cardiomyocytes.[37] In addition, involvement of telomere dysfunction induced p53 upregulation in the development of HF has been suggested.[38,39] Although not all reports support these findings,[40] accumulating evidence indicates that p53 plays an important role in stress-induced apoptosis in the heart.

Roles of p53 in the Development of HF

Several studies have been conducted to clarify the roles of p53 in the development of HF. Many studies indicate that suppressing the function of p53 induces preferable effects on cardiac function. The function of p53 was attenuated by knocking out p53[3] or PUMA,[41] which mediates the proapoptotic effects of p53, and overexpressing MDM2,[33] which induces the ubiquitination and downregulation of p53. An examination of these models showed that these direct or indirect changes in p53 function resulted in decreased cardiomyocyte apoptosis, reduced myocardial infarct size, or a better survival rate after myocardial infarction. In addition, p53-deficient mice have decreased susceptibility to anthracycline-induced myocardial apoptosis and HF.[42] On the other hand, knock-out mice for MDM4, which inhibits the accumulation of p53, develop cardiomyopathy.[43] In addition, overexpressing CHIP, which induces the degradation of p53, attenuated the accumulation of p53 and reduced cardiomyocyte apoptosis after myocardial infarction.[4] These findings indicate that p53 promotes the deterioration of cardiac function.

Recently, both apoptosis and inhibited angiogenesis were suggested to lead to the harmful effects of p53 on cardiac function. In a pressure overloaded mouse model, the cardiac condition transitions from an initial compensatory hypertrophy state to decompensatory HF several weeks after aortic banding. During this transition, p53 is upregulated, hypoxia-inducible factor-1 (HIF-1) expression is attenuated, and microvessels are reduced in the heart. HIF-1 is an established and major inducer of angiogenesis, and p53 was shown to play a pivotal role in downregulating HIF-1 expression during this transition.[5,44]

Potential Crosstalk Between the β-AR-Mediated Signaling Pathway and the p53-Mediated Signaling Pathway

Although there are only a few reports on the relationship between β-AR stimulation and the p53 expression level, p53 was shown to be upregulated in the presence of isoproterenol

in rat cultured cardiomyocytes.[45] In addition, p53 mRNA was also upregulated in cardiomyocytes that were isolated from a murine heart after long-term β-AR stimulation.[46]

On the other hand, p53 affects the expression level or activity of several molecules that can be involved in β-AR-mediated proapoptotic signal transduction, such as GSK-3β and HIF-1.

Accumulated findings obtained from studies of each pathway indicate that there are several possible cross-talk points between the β-AR- and p53-mediated signaling pathways during the induction of apoptosis (**Figure 3**).

Glycogen Synthase Kinase-3β (GSK-3β)

GSK-3β is a Ser/Thr protein kinase that phosphorylates and regulates many molecules that have a role in cell death, cell proliferation, cell growth, etc.[47] Several reports indicate that GSK-3β has proapoptotic effects in cardiomyocytes.[48] GSK-3β phosphorylates p53 and Bax, which facilitates proapoptotic signaling. In addition, 1 study reported that GSK-3β had a proapoptotic role in the isoproterenol-induced apoptosis of cultured adult rat cardiomyocytes.[49] These findings suggest that GSK-3β may have an important role in β-adrenergic signaling-induced p53 activation. On the other hand, GSK-3β can be inactivated via PKA- and AKT-mediated phosphorylation, which can be facilitated by the β-adrenergic signaling pathway.[50] Therefore, in contrast, β-AR stimulation can mediate antiapoptotic effects through GSK-3β. Although the mechanism by which β-AR stimulation induces apoptosis through the GSK-3β pathway is still unclear, studies suggest that a potent GSK-3β-activating pathway can overcome the effect on PKA- and AKT-mediated GSK-3β phosphorylation.

Phosphatase and Tensin Homolog (PTEN)–AKT–MDM2–p53 Loop

AKT (also known as protein kinase B) is involved in the development of hypertrophy, contractility, cell survival and inhibition of apoptosis in cardiomyocytes. The role of AKT in the heart was examined by developing a mouse model in which active AKT is specifically overexpressed in the heart. These mice had cardiac hypertrophy, increased contractility,[51] reduced infarct size and apoptosis after ischemia/reperfusion.[52] AKT is activated upon β-AR stimulation through PI3K and CaMK.[50] Therefore, β-AR stimuli-induced AKT activation may have a negative role in β-AR-induced apoptosis. Although β-AR signaling induces AKT activation through $G\beta\gamma$, at the same time $Gs\alpha$ that is also released from β-AR can inactivate AKT by inhibiting the membrane translocation of phosphoinositide-dependent protein kinase 1 (PDK1).[53] The expression levels of the molecules that are involved in these β-AR-induced pathways, including AC, are thought to be one of the deciding factors of the consequential effects on the role of these β-AR-induced pathways in AKT activity.[54]

AKT inhibits the accumulation of p53 by activating MDM2. When MDM2 is phosphorylated by AKT, MDM2 is translocated into the nucleus and promotes the degradation of p53. On the other hand, p53 inactivates AKT by transactivating PTEN. PTEN is a phosphatidylinositide phosphatase and a known antitumor molecule that inhibits AKT. PTEN overexpression causes apoptosis accompanied by AKT inactivation in cardiomyocytes.[55] Through this positive feedback loop (PTEN–AKT–MDM2–p53 loop),[56] β-AR-induced antiapoptotic signaling via AKT and p53-mediated proapoptotic signaling may eventually negatively affect each other. Regarding the β-AR-induced and p53-induced proapoptotic effects, p53 promotes β-AR-induced apoptosis, while β-AR signaling may inhibit p53-induced apoptosis through the signaling loop.

Calcineurin and Nuclear Factor of Activated T Cell (NFAT)

NFAT is a transcription factor that induces a number of molecules that cause apoptosis, cardiac hypertrophy, cell cycle control, etc. NFAT is activated by the Ca^{2+}/calmodulin-dependent phosphatase, calcineurin, which dephosphorylates NFAT, causing it to translocate from the cytoplasm to the nucleus. Carcinoma cells were shown to undergo p53-induced apoptosis through the calcineurin-dependent signaling pathway.[57] In addition, a previous report showed that both p53 and NFAT were involved in angiotensin II-induced apoptosis in vascular smooth muscle cells.[57,58] On the other hand, other reports have shown that calcineurin has a pivotal role in β-AR stimuli-induced apoptosis in cardiomyocytes.[26] Thus, calcineurin and NFAT may be involved in both the β-AR- and p53-mediated proapoptotic pathways.

Cyclic AMP Response Element-Binding Protein (CBP)/p300

CBP/p300 functions as a cofactor for several transcription factors, including p53, and facilitates their function. In addition, CBP/p300 was also shown to have histone acetyltransferase (HAT) activity. p53 is activated by CBP/p300 through acetylation.[59] When CBP/p300 activates p53, these 2 molecules form a tripartite complex with CREB. The formation of this complex is facilitated by the phosphorylation of CREB by PKA, CaMK, and protein kinase C.[60,61] PKA and CaMK are activated by β-AR signaling. Taken together, it can be speculated that there may be a situation in which β-adrenergic stimuli affect the p53 induced transactivation through the formation of the CBP/p300–CREB–p53 complex.

HIF-1

HIF-1 expression is induced by hypoxia and it predominantly functions as a transcription factor. HIF-1 transactivates a number of proteins that are involved in angiogenesis, cell proliferation, metabolism, cell survival, apoptosis, etc. HIF-1 can induce not only proapoptotic proteins such as BNIP3 and NIX, but also antiapoptotic proteins such as erythropoietin.[62] In addition, HIF-1 promotes the accumulation of p53 by directly interacting with MDM2.[63] Recent reports indicate that HIF-1 helps preserve cardiac function after hypoxic stress. HIF-1 overexpression attenuated cardiac damage after myocardial ischemia/reperfusion injury in cultured cardiomyocytes and a mouse model.[64,65] Although the enhancement of angiogenesis by HIF-1 is likely to be the important mechanism, several reports suggest that HIF-1 may modulate the apoptotic signal in cardiomyocytes.[66–69] Although the role of HIF-1 in the development of apoptosis is not well elucidated, HIF-1 is thought to be a potential factor in the apoptosis of cardiomyocytes.

HIF-1 expression is upregulated by the PI3K–AKT pathway,[70] which can be activated by $G\beta\gamma$ protein-mediated signaling. In addition, Forskolin, an AC activator that can be activated by Gs protein, also induces HIF-1 expression in cancer cells.[71] On the other hand, some reports indicate that p53 downregulates HIF-1 expression. In addition, this downregulation is inhibited by AKT activation,[72] which can be induced by β-AR stimulation. Taken together, β-AR signaling upregulates, while p53 downregulates HIF-1 expression. Therefore, HIF-1-mediated regulation of apoptosis may be a type of competitive cross-talk between the β-AR- and p53-mediated signaling pathways.

However, only a few reports have examined this pathway in cardiomyocytes, so further studies are required in order to determine the importance of this pathway in the development of HF.

Conclusions

It is crucial to maintain the number of cardiomyocytes in order to maintain the function of a failing heart. Although there have been several attempts to develop therapies that regenerate cardiomyocytes using stem cells or progenitor cells, currently there is not a clinically established method to increase in the number of cardiomyocytes.[73,74] Therefore, preventing cell death in the failing heart is still a promising approach to manage and prevent HF.

In this review, we focused on apoptosis as one mechanism of cell death in the failing heart. The β-AR- and p53-mediated signaling pathways are 2 major inducers of apoptosis. Many approaches, including gene therapy, have been developed to modulate the signaling of these pathways. Considering their effects on apoptosis, controlling these pathways could be a promising strategy to preserve cardiac function.

When attempting to establish HF therapies that modulate signal transduction, there are several important issues to be considered.

First, it is important to determine when and where signaling should be modulated. As the use of β-AR agonists or antagonists to treat HF depends on the disease state, the timing should be considered when modulating the p53 signaling pathways. p53 is a major tumor suppressor and may exacerbate HF by inducing apoptosis and inhibiting angiogenesis. However, p53 may also cause preferable effects on the heart. For example, p53 may inhibit the development of arteriosclerosis.[75] In addition, p53 may prevent the proliferation of vascular smooth muscle cells, which is pivotal in coronary restenosis after stent implantation.[76]

The β-antagonists have several side effects, including bronchial asthma, glucose intolerance, and Raynaud's phenomenon, because they affect tissues other than the heart. To avoid these effects, therapies that modulate specific subtypes of AC are near development.[77] In the same way, we should control p53 function in a tissue-specific manner.

Second, it is important to consider the possibility of cross-talk with other pathways that are involved in the development of HF. Modulating certain signaling pathways may affect others. Understanding the cross-talk among several important pathways would be useful in choosing the time and the method of therapeutic intervention to obtain the maximum effect. In this review, we noted 5 possible cross-talk points between the β-AR- and p53-mediated signaling pathways for apoptosis. Some of these are thought to facilitate another pathway. For example, β-adrenergic signaling may enhance the activity of p53 through several pathways. One of the mechanisms by which β blockers help preserve cardiac function may be by attenuating p53 function. On the other hand, potential points of competitive cross-talk have also been identified. For instance, p53 may downregulate HIF-1, while β-AR signaling may upregulate HIF-1. If there is a situation in which HIF-1 plays a significant role in regulating the apoptosis of cardiomyocytes, understanding these potentially interconnected pathways may lead to the development of more effective therapies that prevent apoptosis. Therefore, it will be important to examine the contribution of each pathway, as well as the cross-talk points under various conditions.

On the whole, to selectively inhibit the cAMP signaling pathway while preserving the PI3K–AKT pathway seems to be effective for inhibiting the apoptosis that is induced by these 2 pathways. This fact reminds us of the β1-selective β blockers. However, many pathways and molecules other than these 2 pathways are involved in the apoptosis of cardiomyocytes. Moreover, many mechanisms other than apoptosis are involved in the pathogenesis of HF. Cell death including necrosis, autophagy as well as Ca^{2+} handling, oxidative stress, metabolic state, etc have been identified as important factors that affect the development of HF. This may be one of the reasons why the advantages of β1-selective β blockers compared with nonselective β blockers for HF therapy seem not to be significant in clinical studies. In the COMET trial, the β1, β2, α1 blocker, carvedilol, extended the longevity of chronic HF patients better than the β1-selective blocker metoprolol.[78] Clarifying the relationships and roles of each signaling pathway in the various phases of HF development will lead to the development of more effective and sound treatments.

References

1. Lloyd-Jones DM, Larson MG, Leip EP, Beiser A, D'Agostino RB, Kannel WB, et al. Lifetime risk for developing congestive heart failure: The Framingham Heart Study. *Circulation* 2002; **106:** 3068–3072.
2. Ishikawa Y, Homcy CJ. The adenylyl cyclases as integrators of transmembrane signal transduction. *Circ Res* 1997; **80:** 297–304.
3. Matsusaka H, Ide T, Matsushima S, Ikeuchi M, Kubota T, Sunagawa K, et al. Targeted deletion of p53 prevents cardiac rupture after myocardial infarction in mice. *Cardiovasc Res* 2006; **70:** 457–465.
4. Naito AT, Okada S, Minamino T, Iwanaga K, Liu ML, Sumida T, et al. Promotion of CHIP-mediated p53 degradation protects the heart from ischemic injury. *Circ Res* 2010; **106:** 1692–1702.
5. Das B, Young D, Vasanji A, Gupta S, Sarkar S, Sen S. Influence of p53 in the transition of myotrophin-induced cardiac hypertrophy to heart failure. *Cardiovasc Res* 2010; **87:** 524–534.
6. Sato M, Jiao Q, Honda T, Kurotani R, Toyota E, Okumura S, et al. Activator of G protein signaling 8 (AGS8) is required for hypoxia-induced apoptosis of cardiomyocytes: Role of G betagamma and connexin 43 (CX43). *J Biol Chem* 2009; **284:** 31431–31440.
7. Kang PM, Haunstetter A, Aoki H, Usheva A, Izumo S. Morphological and molecular characterization of adult cardiomyocyte apoptosis during hypoxia and reoxygenation. *Circ Res* 2000; **87:** 118–125.
8. von Harsdorf R, Li PF, Dietz R. Signaling pathways in reactive oxygen species-induced cardiomyocyte apoptosis. *Circulation* 1999; **99:** 2934–2941.
9. Liao X, Liu JM, Du L, Tang A, Shang Y, Wang SQ, et al. Nitric oxide signaling in stretch-induced apoptosis of neonatal rat cardiomyocytes. *FASEB J* 2006; **20:** 1883–1885.
10. Kuramochi Y, Guo X, Sawyer DB, Lim CC. Rapid electrical stimulation induces early activation of kinase signal transduction pathways and apoptosis in adult rat ventricular myocytes. *Exp Physiol* 2006; **91:** 773–780.
11. Suzuki S, Yokoyama U, Abe T, Kiyonari H, Yamashita N, Kato Y, et al. Differential roles of Epac in regulating cell death in neuronal and myocardial cells. *J Biol Chem* 2010; **285:** 24248–24259.
12. Olivetti G, Abbi R, Quaini F, Kajstura J, Cheng W, Nitahara JA, et al. Apoptosis in the failing human heart. *N Engl J Med* 1997; **336:** 1131–1141.
13. Yano M, Ikeda Y, Matsuzaki M. Altered intracellular Ca^{2+} handling in heart failure. *J Clin Invest* 2005; **115:** 556–564.
14. Packer M, Bristow MR, Cohn JN, Colucci WS, Fowler MB, Gilbert EM, et al. The effect of carvedilol on morbidity and mortality in patients with chronic heart failure: U.S. Carvedilol Heart Failure Study Group. *N Engl J Med* 1996; **334:** 1349–1355.
15. Communal C, Singh K, Pimentel DR, Colucci WS. Norepinephrine stimulates apoptosis in adult rat ventricular myocytes by activation of the beta-adrenergic pathway. *Circulation* 1998; **98:** 1329–1334.
16. Bristow MR, Hershberger RE, Port JD, Gilbert EM, Sandoval A, Rasmussen R, et al. Beta-adrenergic pathways in nonfailing and failing human ventricular myocardium. *Circulation* 1990; **82:** 112–125.

17. Zaugg M, Xu W, Lucchinetti E, Shafiq SA, Jamali NZ, Siddiqui MA. Beta-adrenergic receptor subtypes differentially affect apoptosis in adult rat ventricular myocytes. *Circulation* 2000; **102:** 344–350.
18. Zhu WZ, Zheng M, Koch WJ, Lefkowitz RJ, Kobilka BK, Xiao RP. Dual modulation of cell survival and cell death by beta(2)-adrenergic signaling in adult mouse cardiac myocytes. *Proc Natl Acad Sci USA* 2001; **98:** 1607–1612.
19. Ahmet I, Krawczyk M, Heller P, Moon C, Lakatta EG, Talan MI. Beneficial effects of chronic pharmacological manipulation of beta-adrenoreceptor subtype signaling in rodent dilated ischemic cardiomyopathy. *Circulation* 2004; **110:** 1083–1090.
20. Moniotte S, Kobzik L, Feron O, Trochu JN, Gauthier C, Balligand JL. Upregulation of beta(3)-adrenoceptors and altered contractile response to inotropic amines in human failing myocardium. *Circulation* 2001; **103:** 1649–1655.
21. Gauthier C, Leblais V, Kobzik L, Trochu JN, Khandoudi N, Bril A, et al. The negative inotropic effect of beta3-adrenoceptor stimulation is mediated by activation of a nitric oxide synthase pathway in human ventricle. *J Clin Invest* 1998; **102:** 1377–1384.
22. Stefanelli C, Pignatti C, Tantini B, Stanic I, Bonavita F, Muscari C, et al. Nitric oxide can function as either a killer molecule or an anti-apoptotic effector in cardiomyocytes. *Biochim Biophys Acta* 1999; **1450:** 406–413.
23. Ding B, Abe J, Wei H, Xu H, Che W, Aizawa T, et al. A positive feedback loop of phosphodiesterase 3 (PDE3) and inducible cAMP early repressor (ICER) leads to cardiomyocyte apoptosis. *Proc Natl Acad Sci USA* 2005; **102:** 14771–14776.
24. Tomita H, Nazmy M, Kajimoto K, Yehia G, Molina CA, Sadoshima J. Inducible cAMP early repressor (ICER) is a negative-feedback regulator of cardiac hypertrophy and an important mediator of cardiac myocyte apoptosis in response to beta-adrenergic receptor stimulation. *Circ Res* 2003; **93:** 12–22.
25. Zhu WZ, Wang SQ, Chakir K, Yang D, Zhang T, Brown JH, et al. Linkage of beta1-adrenergic stimulation to apoptotic heart cell death through protein kinase A-independent activation of Ca^{2+}/calmodulin kinase II. *J Clin Invest* 2003; **111:** 617–625.
26. Saito S, Hiroi Y, Zou Y, Aikawa R, Toko H, Shibasaki F, et al. beta-Adrenergic pathway induces apoptosis through calcineurin activation in cardiac myocytes. *J Biol Chem* 2000; **275:** 34528–34533.
27. Grimm M, Brown JH. Beta-adrenergic receptor signaling in the heart: Role of CaMKII. *J Mol Cell Cardiol* 2010; **48:** 322–330.
28. Bos JL. Epac: A new cAMP target and new avenues in cAMP research. *Nat Rev Mol Cell Biol* 2003; **4:** 733–738.
29. O'Connor L, Strasser A, O'Reilly LA, Hausmann G, Adams JM, Cory S, et al. Bim: A novel member of the Bcl-2 family that promotes apoptosis. *EMBO J* 1998; **17:** 384–395.
30. Toledo F, Wahl GM. Regulating the p53 pathway: In vitro hypotheses, in vivo veritas. *Nat Rev Cancer* 2006; **6:** 909–923.
31. Vousden KH, Lu X. Live or let die: The cell's response to p53. *Nat Rev Cancer* 2002; **2:** 594–604.
32. Long X, Boluyt MO, Hipolito ML, Lundberg MS, Zheng JS, O'Neill L, et al. p53 and the hypoxia-induced apoptosis of cultured neonatal rat cardiac myocytes. *J Clin Invest* 1997; **99:** 2635–2643.
33. Toth A, Nickson P, Qin LL, Erhardt P. Differential regulation of cardiomyocyte survival and hypertrophy by MDM2, an E3 ubiquitin ligase. *J Biol Chem* 2006; **281:** 3679–3689.
34. Cesselli D, Jakoniuk I, Barlucchi L, Beltrami AP, Hintze TH, Nadal-Ginard B, et al. Oxidative stress-mediated cardiac cell death is a major determinant of ventricular dysfunction and failure in dog dilated cardiomyopathy. *Circ Res* 2001; **89:** 279–286.
35. Leri A, Claudio PP, Li Q, Wang X, Reiss K, Wang S, et al. Stretch-mediated release of angiotensin II induces myocyte apoptosis by activating p53 that enhances the local renin-angiotensin system and decreases the Bcl-2-to-Bax protein ratio in the cell. *J Clin Invest* 1998; **101:** 1326–1342.
36. Leri A, Liu Y, Malhotra A, Li Q, Stiegler P, Claudio PP, et al. Pacing-induced heart failure in dogs enhances the expression of p53 and p53-dependent genes in ventricular myocytes. *Circulation* 1998; **97:** 194–203.
37. Liu J, Mao W, Ding B, Liang CS. ERKs/p53 signal transduction pathway is involved in doxorubicin-induced apoptosis in H9c2 cells and cardiomyocytes. *Am J Physiol Heart Circ Physiol* 2008; **295:** H1956–H1965.
38. Oh H, Wang SC, Prahash A, Sano M, Moravec CS, Taffet GE, et al. Telomere attrition and Chk2 activation in human heart failure. *Proc Natl Acad Sci USA* 2003; **100:** 5378–5383.
39. Torella D, Rota M, Nurzynska D, Musso E, Monsen A, Shiraishi I, et al. Cardiac stem cell and myocyte aging, heart failure, and insulin-like growth factor-1 overexpression. *Circ Res* 2004; **94:** 514–524.
40. Webster KA, Discher DJ, Kaiser S, Hernandez O, Sato B, Bishopric NH. Hypoxia-activated apoptosis of cardiac myocytes requires reoxygenation or a pH shift and is independent of p53. *J Clin Invest* 1999; **104:** 239–252.
41. Toth A, Jeffers JR, Nickson P, Min JY, Morgan JP, Zambetti GP, et al. Targeted deletion of Puma attenuates cardiomyocyte death and improves cardiac function during ischemia-reperfusion. *Am J Physiol Heart Circ Physiol* 2006; **291:** H52–H60.
42. Shizukuda Y, Matoba S, Mian OY, Nguyen T, Hwang PM. Targeted disruption of p53 attenuates doxorubicin-induced cardiac toxicity in mice. *Mol Cell Biochem* 2005; **273:** 25–32.
43. Xiong S, Van Pelt CS, Elizondo-Fraire AC, Fernandez-Garcia B, Lozano G. Loss of Mdm4 results in p53-dependent dilated cardiomyopathy. *Circulation* 2007; **115:** 2925–2930.
44. Sano M, Minamino T, Toko H, Miyauchi H, Orimo M, Qin Y, et al. p53-induced inhibition of Hif-1 causes cardiac dysfunction during pressure overload. *Nature* 2007; **446:** 444–448.
45. Zhou B, Wu LJ, Tashiro S, Onodera S, Uchiumi F, Ikejima T. Silibinin protects rat cardiac myocyte from isoproterenol-induced DNA damage independent on regulation of cell cycle. *Biol Pharm Bull* 2006; **29:** 1900–1905.
46. Kim KK, Soonpaa MH, Daud AI, Koh GY, Kim JS, Field LJ. Tumor suppressor gene expression during normal and pathologic myocardial growth. *J Biol Chem* 1994; **269:** 22607–22613.
47. Miura T, Miki T. GSK-3β, a therapeutic target for cardiomyocyte protection. *Circ J* 2009; **73:** 1184–1192.
48. Yin H, Chao L, Chao J. Kallikrein/kinin protects against myocardial apoptosis after ischemia/reperfusion via Akt-glycogen synthase kinase-3 and Akt-Bad.14-3-3 signaling pathways. *J Biol Chem* 2005; **280:** 8022–8030.
49. Menon B, Johnson JN, Ross RS, Singh M, Singh K. Glycogen synthase kinase-3beta plays a pro-apoptotic role in beta-adrenergic receptor-stimulated apoptosis in adult rat ventricular myocytes: Role of beta1 integrins. *J Mol Cell Cardiol* 2007; **42:** 653–661.
50. Morisco C, Zebrowski D, Condorelli G, Tsichlis P, Vatner SF, Sadoshima J. The Akt-glycogen synthase kinase 3beta pathway regulates transcription of atrial natriuretic factor induced by beta-adrenergic receptor stimulation in cardiac myocytes. *J Biol Chem* 2000; **275:** 14466–14475.
51. Condorelli G, Drusco A, Stassi G, Bellacosa A, Roncarati R, Iaccarino G, et al. Akt induces enhanced myocardial contractility and cell size in vivo in transgenic mice. *Proc Natl Acad Sci USA* 2002; **99:** 12333–12338.
52. Fujio Y, Nguyen T, Wencker D, Kitsis RN, Walsh K. Akt promotes survival of cardiomyocytes in vitro and protects against ischemia-reperfusion injury in mouse heart. *Circulation* 2000; **101:** 660–667.
53. Kim S, Jee K, Kim D, Koh H, Chung J. Cyclic AMP inhibits Akt activity by blocking the membrane localization of PDK1. *J Biol Chem* 2001; **276:** 12864–12870.
54. Okumura S, Vatner DE, Kurotani R, Bai Y, Gao S, Yuan Z, et al. Disruption of type 5 adenylyl cyclase enhances desensitization of cyclic adenosine monophosphate signal and increases Akt signal with chronic catecholamine stress. *Circulation* 2007; **116:** 1776–1783.
55. Schwartzbauer G, Robbins J. The tumor suppressor gene PTEN can regulate cardiac hypertrophy and survival. *J Biol Chem* 2001; **276:** 35786–35793.
56. Oren M. Decision making by p53: Life, death and cancer. *Cell Death Differ* 2003; **10:** 431–442.
57. Rivera A, Maxwell SA. The p53-induced gene-6 (proline oxidase) mediates apoptosis through a calcineurin-dependent pathway. *J Biol Chem* 2005; **280:** 29346–29354.
58. Min LJ, Mogi M, Tamura K, Iwanami J, Sakata A, Fujita T, et al. Angiotensin II type 1 receptor-associated protein prevents vascular smooth muscle cell senescence via inactivation of calcineurin/nuclear factor of activated T cells pathway. *J Mol Cell Cardiol* 2009; **47:** 798–809.
59. Iyer NG, Ozdag H, Caldas C. p300/CBP and cancer. *Oncogene* 2004; **23:** 4225–4231.
60. Giebler HA, Lemasson I, Nyborg JK. p53 recruitment of CREB binding protein mediated through phosphorylated CREB: A novel pathway of tumor suppressor regulation. *Mol Cell Biol* 2000; **20:** 4849–4858.
61. Li B, Kaetzel MA, Dedman JR. Signaling pathways regulating murine cardiac CREB phosphorylation. *Biochem Biophys Res Commun* 2006; **350:** 179–184.
62. Sowter HM, Ratcliffe PJ, Watson P, Greenberg AH, Harris AL. HIF-1-dependent regulation of hypoxic induction of the cell death factors BNIP3 and NIX in human tumors. *Cancer Res* 2001; **61:**

6669–6673.
63. Chen D, Li M, Luo J, Gu W. Direct interactions between HIF-1 alpha and Mdm2 modulate p53 function. *J Biol Chem* 2003; **278:** 13595–13598.
64. Date T, Mochizuki S, Belanger AJ, Yamakawa M, Luo Z, Vincent KA, et al. Expression of constitutively stable hybrid hypoxia-inducible factor-1alpha protects cultured rat cardiomyocytes against simulated ischemia-reperfusion injury. *Am J Physiol Cell Physiol* 2005; **288:** C314–C320.
65. Kido M, Du L, Sullivan CC, Li X, Deutsch R, Jamieson SW, et al. Hypoxia-inducible factor 1-alpha reduces infarction and attenuates progression of cardiac dysfunction after myocardial infarction in the mouse. *J Am Coll Cardiol* 2005; **46:** 2116–2124.
66. Buhler K, Plaisance I, Dieterle T, Brink M. The human urocortin 2 gene is regulated by hypoxia: Identification of a hypoxia-responsive element in the 3'-flanking region. *Biochem J* 2009; **424:** 119–127.
67. Kakinuma Y, Ando M, Kuwabara M, Katare RG, Okudela K, Kobayashi M, et al. Acetylcholine from vagal stimulation protects cardiomyocytes against ischemia and hypoxia involving additive non-hypoxic induction of HIF-1alpha. *FEBS Lett* 2005; **579:** 2111–2118.
68. Recchia AG, De Francesco EM, Vivacqua A, Sisci D, Panno ML, Ando S, et al. The G protein-coupled receptor 30 is up-regulated by hypoxia-inducible factor-1{alpha} (HIF-1{alpha}) in breast cancer cells and cardiomyocytes. *J Biol Chem* 2010; **286:** 10773–10782.
69. Malhotra R, Tyson DW, Rosevear HM, Brosius FC 3rd. Hypoxia-inducible factor-1alpha is a critical mediator of hypoxia induced apoptosis in cardiac H9c2 and kidney epithelial HK-2 cells. *BMC Cardiovasc Disord* 2008; **8:** 9.
70. Jiang BH, Liu LZ. PI3K/PTEN signaling in angiogenesis and tumorigenesis. *Adv Cancer Res* 2009; **102:** 19–65.
71. Park SY, Kang JH, Jeong KJ, Lee J, Han JW, Choi WS, et al. Norepinephrine induces VEGF expression and angiogenesis by a hypoxia-inducible factor-1alpha protein-dependent mechanism. *Int J Cancer* 2011; **128:** 2306–2316.
72. Choy MK, Movassagh M, Bennett MR, Foo RS. PKB/Akt activation inhibits p53-mediated HIF1A degradation that is independent of MDM2. *J Cell Physiol* 2010; **222:** 635–639.
73. Mignone JL, Kreutziger KL, Paige SL, Murry CE. Cardiogenesis from human embryonic stem cells. *Circ J* 2010; **74:** 2517–2526.
74. Hosoda T, Kajstura J, Leri A, Anversa P. Mechanisms of myocardial regeneration. *Circ J* 2010; **74:** 13–17.
75. Guevara NV, Kim HS, Antonova EI, Chan L. The absence of p53 accelerates atherosclerosis by increasing cell proliferation in vivo. *Nat Med* 1999; **5:** 335–339.
76. Sata M, Tanaka K, Ishizaka N, Hirata Y, Nagai R. Absence of p53 leads to accelerated neointimal hyperplasia after vascular injury. *Arterioscler Thromb Vasc Biol* 2003; **23:** 1548–1552.
77. Iwatsubo K, Minamisawa S, Tsunematsu T, Nakagome M, Toya Y, Tomlinson JE, et al. Direct inhibition of type 5 adenylyl cyclase prevents myocardial apoptosis without functional deterioration. *J Biol Chem* 2004; **279:** 40938–40945.
78. Poole-Wilson PA, Swedberg K, Cleland JG, Di Lenarda A, Hanrath P, Komajda M, et al. Comparison of carvedilol and metoprolol on clinical outcomes in patients with chronic heart failure in the Carvedilol Or Metoprolol European Trial (COMET): Randomised controlled trial. *Lancet* 2003; **362:** 7–13.

J Pharmacol Sci 115, 176 – 181 (2011)

Journal of Pharmacological Sciences

Full Paper

Electrophysiological and Pharmacological Characteristics of Triggered Activity Elicited in Guinea-Pig Pulmonary Vein Myocardium

Akira Takahara[1,*], Takahiko Sugimoto[1], Takuma Kitamura[1], Kiyoshi Takeda[1], Yayoi Tsuneoka[1], Iyuki Namekata[1], and Hikaru Tanaka[1]

[1]*Department of Pharmacology, Toho University Faculty of Pharmaceutical Sciences, Funabashi, Chiba 274-8510, Japan*

Received September 10, 2010; Accepted December 5, 2010

Abstract. The pulmonary vein is known as an important source of ectopic beats, initiating frequent paroxysms of atrial fibrillation. We analyzed electrophysiological and pharmacological characteristics of triggered activity elicited in the isolated pulmonary vein from the guinea pig. Immediately after the termination of train stimulation (pacing cycle length of 100 ms), spontaneous activities accompanied with phase-4 depolarization were detected in 43 out of 45 pulmonary vein preparations. Such triggered activities were not observed in the isolated left atrium. The incidence of triggered activity was higher at a shorter pacing cycle length (100 – 200 ms), and the coupling interval was shorter at a shorter pacing cycle length. Verapamil (1 μM), ryanodine (0.1 μM), and pilsicainide (10 μM) suppressed the occurrence of triggered activities. The resting membrane potential of the pulmonary vein myocardium was more positive than that of the left atrium. Carbachol (0.3 μM) hyperpolarized the resting membrane potential and completely inhibited the occurrence of triggered activities. These results suggest that the pulmonary veins have more arrhythmogenic features than the left atrium, possibly through lower resting membrane potential. The electrophysiological and pharmacological characteristics of triggered activity elicited in the pulmonary vein myocardium were similar to those previously reported using ventricular tissues.

Keywords: triggered activity, pulmonary vein, left atrium, membrane potential, carbachol

Introduction

Atrial fibrillation is known as the most common cardiac arrhythmia in adults, which is a major cause of stroke (1). Whereas the arrhythmia has been recognized to perpetuated by reentrant wavelets propagating in an abnormal atrial-tissue substrate, Haïssaguerre et al. found in 1998 that the origin of atrial ectopic beats was localized in the pulmonary vein myocardial sleeve of patients with drug-resistant atrial fibrillation (2). Cheung reported in 1980 that isolated pulmonary vein preparations from guinea pigs were capable of independent pace-making activity (3). Recently, electrophysiological characteristics of the pulmonary vein have been extensively analyzed in isolated rabbit or dog preparations, which show that the combination of reentrant and non-reentrant mechanisms is the underlying arrhythmogenic mechanisms of atrial fibrillation from the pulmonary veins (4 – 6).

Triggered activity is one of the well-recognized mechanisms of ectopy aggravated by an increased rate of beating (7 – 9). Tactics to raise the intracellular Ca^{2+} concentration of the ventricular tissues, such as treatment with digitalis or a low K^+ / high Ca^{2+} extracellular environment, causes an oscillatory Ca^{2+} release from the sarcoplasmic reticulum and transient depolarization after completion of ventricular repolarization (10). The delayed afterdepolarization (DAD) and resulting triggered activity have been shown to be effectively suppressed by Na^+-channel blockers, Ca^{2+}-channel blockers, and ryanodine in isolated ventricular preparations (11, 12). DAD-related triggered activity has been demonstrated in isolated pulmonary vein myocardium or its isolated cardiomyocytes (13, 14). However, fundamental electrophysiological characteristics of triggered activity have never been examined, such as the relationship between pacing rate to induce triggered activity and its incidence or coupling interval (10). In this study, to better understand the arrhythmogenic activity of the pulmonary vein

*Corresponding author. akirat@phar.toho-u.ac.jp
Published online in J-STAGE on January 18, 2011 (in advance)
doi: 10.1254/jphs.10232FP

itself, we analyzed electrophysiological and pharmacological characteristics of the triggered activity in isolated guinea-pig pulmonary vein. Triggered activity was induced by train stimulation, which is known as a useful methodology to reproducibly induce DAD-related triggered activity (10, 12, 15).

Materials and Methods

All experiments were approved by the Ethics Committee of Toho University Faculty of Pharmaceutical Sciences and performed in accordance with the Guiding Principles for the Care and Use of Laboratory Animals approved by The Japanese Pharmacological Society. The heart and adjunct lungs were isolated from male or female Hartley guinea pigs weighing 350 – 450 g. The pulmonary veins were separated from the left atrium and lung at the end of the pulmonary vein myocardium sleeve in Krebs-Henseleit solution of the following composition: 118.4 mM NaCl, 4.7 mM KCl, 2.5 mM $CaCl_2$, 1.2 mM $MgSO_4$, 1.2 mM KH_2PO_4, 24.9 mM $NaHCO_3$, and 11.1 mM glucose, gassed with 95% O_2 / 5% CO_2 (pH 7.4 at 37°C).

Histological examinations

Pulmonary veins were fixed with 10% formalin neutral buffer solution, and the segments were processed into paraffin blocks. The paraffinized tissue blocks were cut into 4-μm-thick sections and mounted on charged slides. For each paraffin block, one slide each was stained with Masson trichrome to accentuate muscle and connective tissues. A serial section was incubated with antibodies against α-smooth muscle actin (α-SMA, 1:500; Dako, Glostup, Denmark) followed by consecutive incubations with universal immuno-peroxydase polymer (Histofine®, Simple Stain Rat MAX PO MULTI; Nichirei Bioscience, Tokyo). Antibody binding was demonstrated by staining with 3,3'-diaminobenzidine tetrahydrochloride.

Microelectrode recording of action potential configuration

The luminal side of the pulmonary vein at the middle region between the ostium and the distal end of myocardial sleeve or endocardial surface of the left atrium was impaled with glass microelectrodes filled with 3 M KCl to record transmembrane potential using a microelectrode amplifier (Intra 767; World Precision Instruments, Sarasota, FL, USA). The action potential signals were monitored by an oscilloscope (CS-5135; Kenwood, Tokyo) and fed into a waveform analysis system (DSS98-type IV, from Canopus, Tokyo or PowerLab, from ADInstruments, Castle Hill, Australia). All experiments were performed at 36.5 ± 0.5°C.

Triggered activity was induced by a burst pacing of 100 train pulses at a pacing cycle length of 100, 150, or 200 ms using an electronic stimulator (SEN-2201; Nihon Kohden, Tokyo) with rectangular current pulses (3-ms duration, about 1.5 threshold) through bipolar platinum electrodes. Action potential parameters, including resting potential (RP), overshoot (OS), and action potential duration at 20% (APD_{20}), 50% (APD_{50}), and 90% (APD_{90}) repolarization, were measured under electrical stimulation at a constant frequency of 1 Hz. The action potentials of the pulmonary vein were of the fast-response type, and neither early afterdepolarizations (EADs) nor DADs were observed in the preparations electrically driven at 1 Hz.

Drugs

Verapamil hydrochloride and carbachol were purchased from Sigma-Aldrich (St. Louis, MO, USA), and ryanodine was obtained from Wako (Osaka). Pilsicainide hydrochloride was kindly provided by Daiichi-Sankyo Co., Ltd. (Tokyo). Ryanodine was initially dissolved in dimethylsulfoxide and diluted to 0.01% dimethylsulfoxide in the Krebs-Henseleit solution. Other drugs were dissolved in distilled water and small aliquots were added to the organ bath to obtain the desired final concentration. All other chemicals were commercial products of the highest available quality.

Statistical analyses

Statistical significance between means was evaluated by the one-way repeated measures analysis of variance followed by Contrasts for mean values comparison or by Dunnett's test. A P-value less than 0.05 was considered significant.

Results

Histology of the pulmonary vein

Typical photomicrographs of longitudinal sections of the left superior pulmonary vein obtained from the guinea pig are shown in Fig. 1. Vascular smooth muscle was detected on the luminal face of the pulmonary vein, whereas a myocardial sleeve was observed at mid-layer of the pulmonary vein.

Triggered activities in the pulmonary vein

Figure 2A shows a typical tracing of burst pacing-induced triggered activity in the pulmonary vein preparation. After the train stimulation at a pacing cycle length of 100 ms, spontaneous activities accompanied with phase-4 depolarization were detected in 43 out of 45 pulmonary vein preparations. On the other hand, phase-4 depolarization was not detected in the left atrium prepa-

rations examined (n = 8). As shown in the Table 1, the incidence of triggered activity and number of premature beats were greater after the faster train stimulation. The coupling interval decreased in a frequency-dependent manner.

Effects of pharmacological intervention on the triggered activity

At the pre-drug period, the number of triggered activity, which was induced after the 100-train stimulation at a pacing cycle length of 100 ms, was 2.4 ± 0.2 in the control group, 2.6 ± 0.9 in the pilsicainide group, 2.4 ± 0.7 in the ryanodine group, and 2.4 ± 0.4 in the verapamil group. There were no significant differences

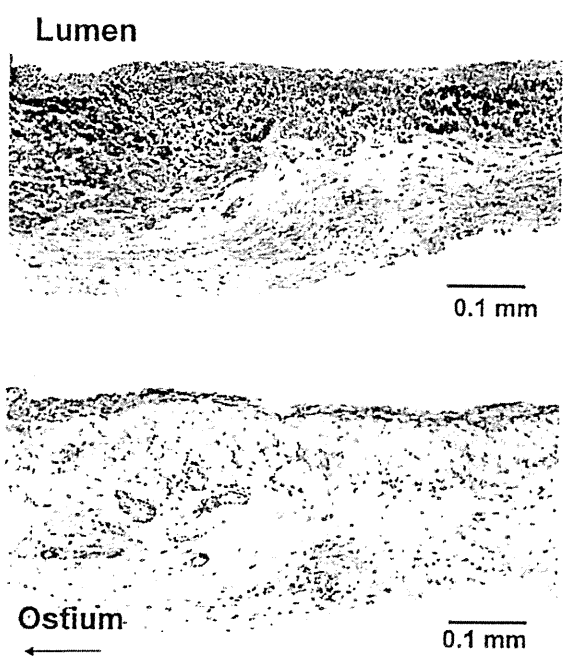

Fig. 1. Photomicrograghs of longitudinal sections of the left superior pulmonary vein of the guinea pig. Upper panel: masson trichrome staining. Lower panel: immunostaining for α-smooth muscle actin (α-SMA).

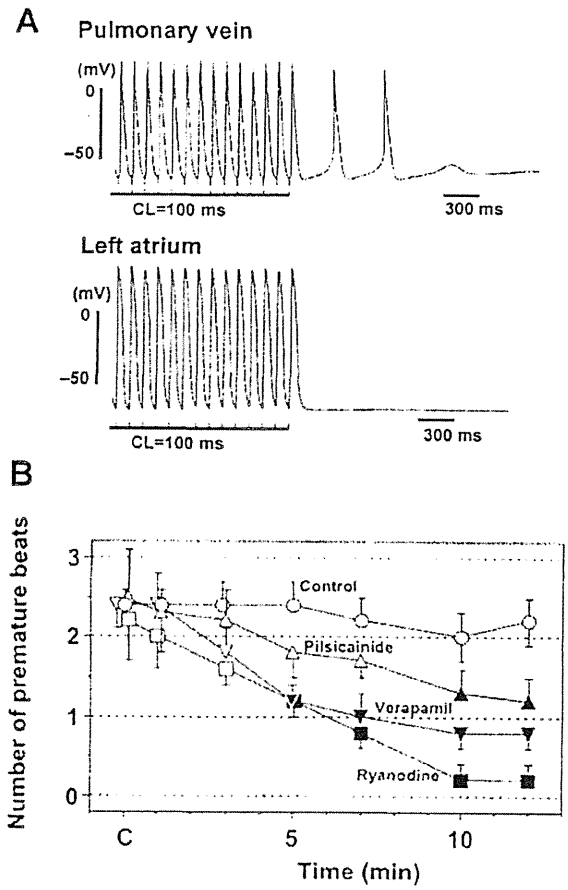

Fig. 2. Delayed afterdepolarization (DAD)-related triggered activity induced by train stimulation. A: A typical tracing of DAD-related triggered activity recorded from the pulmonary vein myocardium after the train stimulation at a pacing cycle length of 100 ms. Two premature beats were detected in this preparation. The DAD-related triggered activity was not observed in the left atrium. B: Summary of the effects of pilsicainide, verapamil, and ryanodine on the number of premature beats in the pulmonary vein preparation. Train stimulation (CL = 100 ms) was applied to the preparation before (C) and at 1, 3, 5, 7, 10, and 12 min after the drug administration. Data are means ± S.E.M. Pilsicainide: 10 μM (n = 6), verapamil: 1 μM (n = 5), ryanodine: 0.1 μM (n = 5), and control (n = 5). Closed symbols represent significant differences from the corresponding pre-drug values (C) at $P < 0.05$. CL: cycle length.

Table 1. Frequency-dependent induction of the triggered activity in pulmonary vein

Pacing cycle length	Pulmonary vein			Left atrium
	200 ms	150 ms	100 ms	100 ms
Incidence	18/45 (40.0%)	33/45 (73.3%)	43/45 (95.6%)	0/8 (0%)
Number of premature beats	0.7 ± 0.1	1.4 ± 0.2*	2.1 ± 0.2*	0 ± 0
Coupling interval (ms)	613 ± 24	564 ± 18	490 ± 16*	–

Data are means ± S.E.M. *$P < 0.05$, compared with the corresponding values at a pacing cycle length of 200 ms.

among the groups. The number of triggered activity was unchanged during the observation period in the absence of drugs (control), whereas it was significantly decreased by pilsicainide at 10 μM, verapamil at 1 μM, and ryanodine at 0.1 μM, as shown in the Fig. 2B.

Effects of carbachol on the triggered activity

At the pre-drug period, the number of triggered activity was 2.2 ± 0.5 in the carbachol group. Carbachol at 0.3 μM decreased the number of triggered activity, as shown in the Fig. 3. The same concentration of carbachol shortened the action potential duration of the left atrium electrically driven at 1 Hz without affecting the resting membrane potential, as shown in Table 2. On the other hand, carbachol shortened the action potential duration of the pulmonary vein myocardium together with significant hyperpolizing effects on the resting membrane potential.

Discussion

In this study, we investigated the inducibility of triggered activity in the guinea-pig pulmonary vein myocardium, which is distributed at the mid-layer of the pulmonary vein tissue, as shown in Fig. 1. The shorter pacing cycle length (100 ms) of train stimulation provoked triggered activity in the pulmonary vein preparation, whereas such phenomenon was not observed in the left atrial preparations (Fig. 2A). In previous studies using isolated ventricular tissues, triggered activity is often induced by train stimulation in the presence of intracellular Ca^{2+} overload by using cardiac glycoside or low K^+ / high Ca^{2+} extracellular solution (10, 12, 15). In this study, however, the triggered activity could be induced in the pulmonary vein preparation under the normal experimental condition consisting of a standard physiological solution without cardiac glycoside, as shown in Fig. 2A. These results suggest that the pulmonary vein prepara-

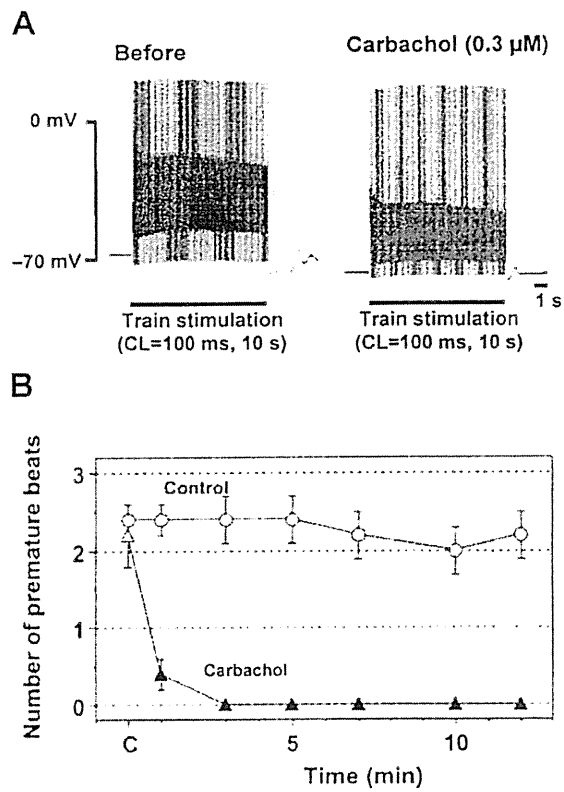

Fig. 3. Effects of carbachol on the DAD-related triggered activity elicited in the pulmonary vein preparation. A: Typical tracings of effects of carbachol on the DAD potentials after the train stimulation at a pacing cycle length of 100 ms. B: Summary of the effects of carbachol (0.3 μM, n = 5) on the number of premature beats. Train stimulation (CL = 100 ms) was applied to the preparation before (C) and at 1, 3, 5, 7, 10, and 12 min after the drug administration. Data are means ± S.E.M. Closed symbols represent the significant differences from corresponding pre-drug values (C) by $P < 0.05$.

Table 2. Effects of carbachol (0.3 μM) on the action potential parameters of the pulmonary vein and left atrium

	Pulmonary vein		Left atrium	
	Before	Carbachol	Before	Carbachol
RP (mV)	−70.3 ± 1.0	−75.4 ± 0.9*	−80.6 ± 1.1	−80.0 ± 0.6
OS (mV)	27.9 ± 2.3	26.4 ± 1.4	27.1 ± 0.8	18.2 ± 1.4*
APD_{20} (ms)	13.2 ± 0.6	9.8 ± 0.5*	23.3 ± 1.2	12.7 ± 0.8*
APD_{50} (ms)	28.0 ± 1.9	18.9 ± 1.1*	40.7 ± 1.6	21.3 ± 1.1*
APD_{90} (ms)	75.5 ± 2.5	57.6 ± 3.5*	76.1 ± 2.7	45.5 ± 1.9*

Data are means ± S.E.M. of 5 experiments. The preparations were electrically driven at 1 Hz. Resting potential (RP); overshoot (OS); action potential duration at 20% (APD_{20}), 50% (APD_{50}), and 90% (APD_{90}) repolarization. *$P < 0.05$, compared with the corresponding control values (Before).

tion has more arrhythmogenic characteristics than the ventricular tissues and the left atria of this study.

Next, we analyzed electrophysiological and pharmacological characteristics of triggered activity elicited in the guinea-pig pulmonary vein myocardium. The higher incidence of triggered activity and the shortening of coupling interval were detected in a frequency-dependent manner, as summarized in Table 1, which is in accordance with earlier literature demonstrating typical electrophysiological features of the DAD-related triggered activity in the ventricular tissues (10). As shown in the Fig. 2B, optimum concentrations of pilsicainide and verapamil (15, 16) effectively inhibited the occurrence of triggered activity in the pulmonary vein preparation, suggesting that inhibition of Na^+ and Ca^{2+} influx through voltage-dependent channels might relieve Ca^{2+} accumulation in the pulmonary vein cardiomyocytes induced by train stimulation. In this study, ryanodine at 0.1 μM, which suppressed ouabain-induced excitability in the guinea-pig pulmonary vein (17), effectively inhibited occurrence of train stimulation–induced triggered activity. On the other hand, Honjo et al. have demonstrated that 0.5 – 2 μM of ryanodine promoted occurrence of triggered activity in rabbit pulmonary vein preparations (13). Ryanodine has been known to have a unique pharmacological profile that can either stimulate or inhibit Ca^{2+} release, depending on the experimental conditions including its concentration or incubation time (18). Taken together, these observations at least suggest that generation of the train stimulation–induced triggered activity is closely associated with oscillatory Ca^{2+} release from the sarcoplasmic reticulum, leading to transient depolarization after completion of ventricular repolarization (10). Each of the drugs used in this study has been demonstrated to suppress train stimulation–induced triggered activity in the canine ventricular tissues intoxicated with cardiac glycoside (12). Therefore, these results suggest that electrophysiological and pharmacological characteristics of triggered activity elicited in the pulmonary vein myocardium were fundamentally similar to those previously reported in the ventricular tissues (10, 12), which may be important information on the therapeutic strategy for the triggered activity elicited in the pulmonary vein myocardium.

It is known that the pulmonary vein as well as the atrium is densely innervated by the autonomic nerves (19, 20), and parasympathetic nerve activation usually encourages reentry via shortening of the effective refractory period, acting as a maintenance factor of atrial fibrillation. Indeed, in the canine model of vagally induced atrial fibrillation, ablation of the autonomic ganglia near the ostia of pulmonary vein prevented atrial fibrillation, showing the importance of cholinergic activation in the pulmonary veins for this type of atrial fibrillation (21). On the other hand, information is still limited regarding the influence of muscarinic receptor activation on the occurrence of triggered activity, as an initiation factor of atrial fibrillation. As shown in Fig. 3, application of carbachol to the pulmonary vein preparation hyperpolarized the resting membrane potential and potently suppressed the train stimulation–induced triggered activity. These results imply that parasympathetic nerve activation may act differently on atrial fibrillation, depending on the type or underlying mechanisms of atrial fibrillation.

In this study, triggered activity could be induced by train stimulation in the pulmonary vein preparation under the normal experimental condition, whereas ventricular cells usually exhibit triggered activity under pathological conditions (10, 12, 15). Previous studies using the isolated cardiomyocytes from the pulmonary vein myocardium have demonstrated that the density of inward rectifier current (I_{K1}) was about half of that in the left atrial cells, which is potentially accounting for the less negative resting membrane potentials in the pulmonary vein myocardium (22, 23). As shown in Table 2, application of carbachol to the pulmonary vein myocardium hyperpolarized the membrane potential through increment of G protein–activated inward-rectifier currents (24), which might contribute a decrease of cell excitability, leading to counteraction of the train stimulation–induced triggered activity (Fig. 3). Thus, it is speculated that arrhythmogenicity of the pulmonary vein myocardium is closely associated with its lower resting membrane potential, which may explain the induction of triggered activity under the normal experimental condition.

In conclusion, these results suggest that the pulmonary vein has more arrhythmogenic features than the left atrium possibly through lower resting membrane potential. The electrophysiological and pharmacological characteristics of triggered activity elicited in the pulmonary vein myocardium were fundamentally similar to those previously reported using the ventricular tissues.

Acknowledgments

This study was supported in part by a Grant-in-Aid from the Ministry of Education, Culture, Sports, Science, and Technology of Japan (#21590602); the Pharmacological Research Foundation (Tokyo); the Science Research Promotion Fund from the Promotion and Mutual Aid Corporation for Private Schools of Japan; and "Research on the molecular mechanisms of appearance of age-related diseases by failure of cell function control system, and their prevention and treatment" by the "Research Center for Aging and Age-related Diseases" established in the Toho University Faculty of Pharmaceutical Sciences.

References

1 Kaarisalo MM, Immonen-Räihä P, Marttila RJ, Salomaa V, Kaarsalo E, Salmi K, et al. Atrial fibrillation and stroke. Mortality and causes of death after the first acute ischemic stroke. Stroke. 1997;28:311–315.

2 Haïssaguerre M, Jaïs P, Shah DC, Takahashi A, Hocini M, Quiniou G, et al. Spontaneous initiation of atrial fibrillation by ectopic beats originating in the pulmonary veins. N Engl J Med. 1998;339:659–666.

3 Cheung DW. Electrical activity of the pulmonary vein and its interaction with the right atrium in the guinea-pig. J Physiol. 1981; 314:445–456.

4 Chen YJ, Chen SA, Chang MS, Lin CI. Arrhythmogenic activity of cardiac muscle in pulmonary veins of the dog: implication for the genesis of atrial fibrillation. Cardiovasc Res. 2000;48: 265–273.

5 Chen YC, Chen SA, Chen YJ, Tai CT, Chan P, Lin CI. T-type calcium current in electrical activity of cardiomyocytes isolated from rabbit pulmonary vein. J Cardiovasc Electrophysiol. 2004; 15:567–571.

6 Wang TM, Luk HN, Sheu JR, Wu HP, Chiang CE. Inducibility of abnormal automaticity and triggered activity in myocardial sleeves of canine pulmonary veins. Int J Cardiol. 2005;104: 59–66.

7 Vermeulen JT, McGuire MA, Opthof T, Coronel R, de Bakker JM, Klopping C, et al. Triggered activity and automaticity in ventricular trabeculae of failing human and rabbit hearts. Cardiovasc Res. 1994;28:1547–1554.

8 De Bakker JM, Ho SY, Hocini M. Basic and clinical electrophysiology of pulmonary vein ectopy. Cardiovasc Res. 2002;54: 287–294.

9 Wit A, Cranefield P. Triggered and automatic activity in the canine coronary sinus. Circ Res. 1977;41:435–445.

10 Hiraoka M. Characteristics of triggered-activity and delayed afterdepolarization in responses to the electrical stimulation. Jpn Circ J. 1987;51:176–180.

11 Rosen MR, Danilo P Jr. Effects of tetrodotoxin, lidocaine, verapamil, and AHR-2666 on ouabain-induced delayed afterdepolarizations in canine Purkinje fibers. Circ Res. 1980;46:117–124.

12 Sugiyama A, Hashimoto K. Can the MAP technique be applied to detect delayed afterdepolarization? Electrophysiologic and pharmacologic evidence. J Cardiovasc Pharmacol. 1999;34: 46–52.

13 Honjo H, Boyett MR, Niwa R, Inada S, Yamamoto M, Mitsui K, et al. Pacing-induced spontaneous activity in myocardial sleeves of pulmonary veins after treatment with ryanodine. Circulation. 2003;107:1937–1943.

14 Chen YJ, Chen SA, Chen YC, Yeh HI, Chan P, Chang MS, et al. Effects of rapid atrial pacing on the arrhythmogenic activity of single cardiomyocytes from pulmonary veins: implication in initiation of atrial fibrillation. Circulation. 2001;104:2849–2854.

15 Inomata N, Ishihara T. Mechanism of inhibition by SUN 1165, a new Na channel blocking antiarrhythmic agent, of cardiac glycoside-induced triggered activity. Eur J Pharmacol. 1988;145: 313–322.

16 Noguchi K, Masumiya H, Takahashi K, Kaneko K, Higuchi S, Tanaka H, et al. Comparative effects of gallopamil and verapamil on the mechanical and electrophysiological parameters of isolated guinea-pig myocardium. Can J Physiol Pharmacol. 1997;75: 1316–1321.

17 Namekata I, Tsuneoka Y, Takahara A, Shimada H, Sugimoto T, Takeda K, et al. Involvement of the Na^+/Ca^{2+} exchanger in the automaticity of guinea-pig pulmonary vein myocardium as revealed by SEA0400. J Pharmacol Sci. 2009;110:111–116.

18 Zucchi R, Ronca-Testoni S. The sarcoplasmic reticulum Ca^{2+} channel/ryanodine receptor: modulation by endogenous effectors, drugs and disease states. Pharmacol Rev. 1997;49:1–51.

19 Tan AY, Li H, Wachsmann-Hogiu S, Chen LS, Chen PS, Fishbein MC. Autonomic innervation and segmental muscular disconnections at the human pulmonary vein-atrial junction: implications for catheter ablation of atrial-pulmonary vein junction. J Am Coll Cardiol. 2006;48:132–143.

20 Arora R, Ng J, Ulphani J, Mylonas I, Subacius H, Shade G, et al. Unique autonomic profile of the pulmonary veins and posterior left atrium. J Am Coll Cardiol. 2007;49:1340–1348.

21 Lemola K, Chartier D, Yeh YH, Dubuc M, Cartier R, Armour A, et al. Pulmonary vein region ablation in experimental vagal atrial fibrillation: role of pulmonary veins versus autonomic ganglia. Circulation. 2008;117:470–477.

22 Ehrlich JR, Cha TJ, Zhang L, Chartier D, Melnyk P, Hohnloser SH, et al. Cellular electrophysiology of canine pulmonary vein cardiomyocytes: action potential and ionic current properties. J Physiol. 2003;551:801–813.

23 Pogwizd SM, Schlotthauer K, Li L, Yuan W, Bers DM. Arrhythmogenesis and contractile dysfunction in heart failure: roles of sodium-calcium exchange, inward rectifier potassium current, and residual β-adrenergic responsiveness. Circ Res. 2001;88: 1159–1167.

24 Tanaka H, Namekata I, Nouchi H, Shigenobu K, Kawanishi T, Takahara A. New aspects for the treatment of cardiac diseases based on the diversity of functional controls on cardiac muscles: diversity in the excitation-contraction mechanisms of the heart. J Pharmacol Sci. 2009;109:327–333.

J Pharmacol Sci 115, 235 – 238 (2011)

Journal of Pharmacological Sciences

Short Communication

Developmental Changes in Action Potential Prolongation by K^+-Channel Blockers in Chick Myocardium

Hideaki Nouchi[1], Naoaki Kiryu[1], Mikio Kimata[1], Yayoi Tsuneoka[1], Shogo Hamaguchi[1], Iyuki Namekata[1,*], Akira Takahara[1], Koki Shigenobu[1], and Hikaru Tanaka[1]

[1]*Department of Pharmacology, Toho University Faculty of Pharmaceutical Sciences, Miyama 2-2-1, Funabashi, Chiba 274-8510, Japan*

Received August 7, 2010; Accepted December 12, 2010

Abstract. The effects of K^+-channel blockers on the action potential duration of the myocardium were examined in isolated right ventricles from the 7 – 10-day-old, 11 – 13-day-old, and 14 – 20-day-old embryo and 1 – 7-day-old hatched chicks. E-4031 significantly prolonged action potential duration at all developmental stages examined; the prolongation was largest in the 11 – 13-day-old embryo and was accompanied by early after-depolarizations. Chromanol 293B showed smaller prolongation at all stages examined. Terfenadine prolonged action potential duration in the 11 – 13-day-old embryo, but not in other stages. Thus, the chick ventricular myocardium changes its repolarization properties during development.

Keywords: chick, K^+-channel blocker, action potential duration

The chick embryo heart has been used to study various aspects of myocardial excitation and contraction. Although the chick heart shares common basic mechanisms with the mammalian heart, characteristic features in the electrophysiological properties, Ca^{2+} handling, contraction, and their physiological and pharmacological regulation has been reported (1 – 4). Concerning its electrophysiological properties, the resting membrane potential and action potential amplitude was reported to increase progressively during embryonic development (1), and many reports have been published concerning the depolarizing membrane currents involved (2). On the other hand, relatively little is known about its repolarization process, which is the determinant of the action potential duration. In the case of mammalian myocardia, information on the species difference and developmental changes in repolarization properties have accumulated, which enables appropriate selection of preparations for different experimental purposes (4). In the present study, we intended to obtain information about the repolarization mechanisms of the chick heart. We applied standard microelectrode techniques to the chick embryonic ventricular myocardia from four different developmental stages and examined the effect of inhibitors of the delayed rectifier potassium current, the major repolarizing current in the myocardium.

Standard microelectrode experiments were performed as previously described (5 – 7). Briefly, fertilized chicken eggs were incubated at 37°C, and the right ventricular free wall was isolated from 7 – 10-day-old embryo, 11 – 13-day-old embryo, 14 – 20-day-old embryo, and 1 – 7-day-old hatched chicks. They were driven at 1 Hz in an organ bath containing physiological salt solution of the following composition: 118.4 mM NaCl, 4.7 mM KCl, 2.5 mM $CaCl_2$, 1.2 mM $MgCl_2$, 1.2 mM KH_2PO_4, 24.9 mM $NaHCO_3$, and 11.1 mM glucose. The solution was gassed with 95% O_2 – 5% CO_2 and maintained at 37°C (pH 7.4). All experimental data are expressed as the mean ± S.E.M., and statistical significance of differences between means were evaluated by the paired *t*-test. A P value less than 0.05 were considered significant. The drugs used were E-4031 (Wako, Osaka), chromanol 293B (Sigma, St. Louis, MO, USA), and terfenadine (Wako). All other drugs and chemicals were commercial products of the highest available quality.

The resting potential, overshoot and the maximum rate of rise increased progressively during the embryonic period (Table 1, Fig. 1A). Action potential duration increased progressively during the embryonic period. The action potential duration of 1 – 7-day-old hatched chicks

*Corresponding author. iyuki@phar.toho-u.ac.jp
Published online in J-STAGE on January 20, 2011 (in advance)
doi: 10.1254/jphs.10205SC

Table 1. Developmental changes in action potential parameters

Parameters (units)	7 – 10-day-old embryo	11 – 13-day-old embryo	14 – 20-day-old embryo	1 – 7-day-old hatched chicks
RP (mV)	−78.8 ± 0.3	−80.8 ± 0.4	−82.4 ± 0.3	−82.8 ± 0.3
OS (mV)	34.4 ± 0.5	36.7 ± 0.4	37.7 ± 0.5	37.3 ± 0.3
APD_{20} (ms)	103.1 ± 2.7	103.4 ± 2.8	106.9 ± 2.9	102.3 ± 2.7
APD_{50} (ms)	152.8 ± 3.0	154.3 ± 2.7	163.9 ± 2.6	145.5 ± 2.8
APD_{90} (ms)	180.4 ± 2.6	185.6 ± 2.6	197.8 ± 1.7	168.5 ± 2.8
$\dot{V}_{max}$ (V/s)	118.2 ± 6.3	149.3 ± 8.4	180.1 ± 4.1	177.8 ± 3.7

Action potential parameters of ventricular myocardia from 7 – 10-day-old embryos, 11 – 13-day-old embryos, 14 – 20-day-old embryos, and 1 – 7-day-old hatched chicks were obtained in the absence of agents. RP, OS, and $\dot{V}_{max}$ indicate resting potential, overshoot, and maximum rate of phase-0 depolarization, respectively. APD_{20}, APD_{50}, and APD_{90} indicate action potential duration at 20%, 50%, and 90% repolarization, respectively. Each value is the mean ± S.E.M. from 36 experiments.

was shorter than that of the 14 – 20-day-old embryos.

E-4031 (1 μM), a blocker of I_{Kr}, significantly prolonged action potential duration at all developmental stages (Fig. 1: A, Ca). The magnitude of prolongation by E-4031 was larger in 7 – 10-day-old embryo and 11 – 13-day-old embryo than in the 14 – 20-day-old embryo and 1 – 7-day-old hatched chick. In the 11 – 13-day-old embryo, the prolongation by E-4031 was prominent and was accompanied by early after-depolarizations (EADs); phase 3 repolarization was interrupted followed by a single or a series of partial depolarization toward 0-mV level (Fig. 1Ac). Early after-depolarizations were observed in all of the preparations from the 11 – 13-day-old embryo (n = 6), but was not observed in those from other stages.

Chromanol 293B (30 μM), a blocker of the slowly activating component of the delayed rectifier K^+ current (I_{Ks}), prolonged action potential duration at all developmental stages (Fig. 1Cb); the prolongation by chromanol 293B was statistically significant, but was much smaller than that by E-4031 at all developmental stages.

Terfenadine (30 μM) produced a prolongation of the action potential duration in the 11 – 13-day-old embryo. Such prolongation was not observed at other stages (Fig. 1B, Cc).

The action potential duration of the chick ventricular myocardium increased during the embryonic period and was shortened in the hatched chick. This was in agreement with previous reports (1, 8) and also appeared to be similar to the case in the guinea pig where the action potential duration increased during the embryonic period followed by a decrease during the perinatal period (9). The developmental change in action potential duration is likely to be accompanied by changes in the balance of underlying membrane currents, as was shown to be the case in guinea pig (10). Such changes would greatly affect the responsiveness of the myocardium to pharmacological agents acting on myocardial ion channels. E-4031 markedly prolonged the action potential duration at all ages examined, while the prolongation by chromanol 293B was small (Fig. 1C). This suggests that in the chick ventricular myocardium, the rapid component (I_{Kr}), but not the slow component (I_{Ks}), of the delayed rectifier potassium channel is largely responsible for the repolarization, which is the same as in many mammalian species including the guinea pig, rabbit, and human. The prolongation by E-4031 was most prominent in the 11 – 13-day-old embryo (Fig. 1). The most likely explanation is that the prolongation of the repolarization phase of the embryonic myocardia reflects less density of repolarizing currents. In other words, the embryonic myocardia have less "repolarization reserve" (11), which makes the action potential highly sensitive to I_{Kr} blockade. Early afterdepolarizations, which are considered to be one of the causes of cardiac arrhythmia, were induced by E-4031 in all of the preparations from the 11 – 13-day-old embryo (Fig. 1Ac). In mammalian myocardia, I_{Kr} blockade is known to induce action potential prolongation, but does not always induce early after-depolarization. For example, in guinea-pig ventricular myocardium, E-4031 (1 μM) prolonged the action potential duration by about 70 ms, but did not induce early after-depolarizations (12).

Clinical treatment with certain cardiovascular and non-cardiovascular drugs has been reported to induce QT prolongation and serious ventricular arrhythmia including *torsades de pointes*. Drugs such as terfenadine and cisapride were withdrawn from clinical practice because of their arrhythmogenic risk. Since then, the assessment of the risks incurred with noncardiovascular therapeutic agents for cardiac function has received great attention (13). Terfenadine inhibits the I_{Kr} current in freshly isolated myocardial cells (14) and the hERG channel current expressed in HEK293 cells (15), but does not prolong the

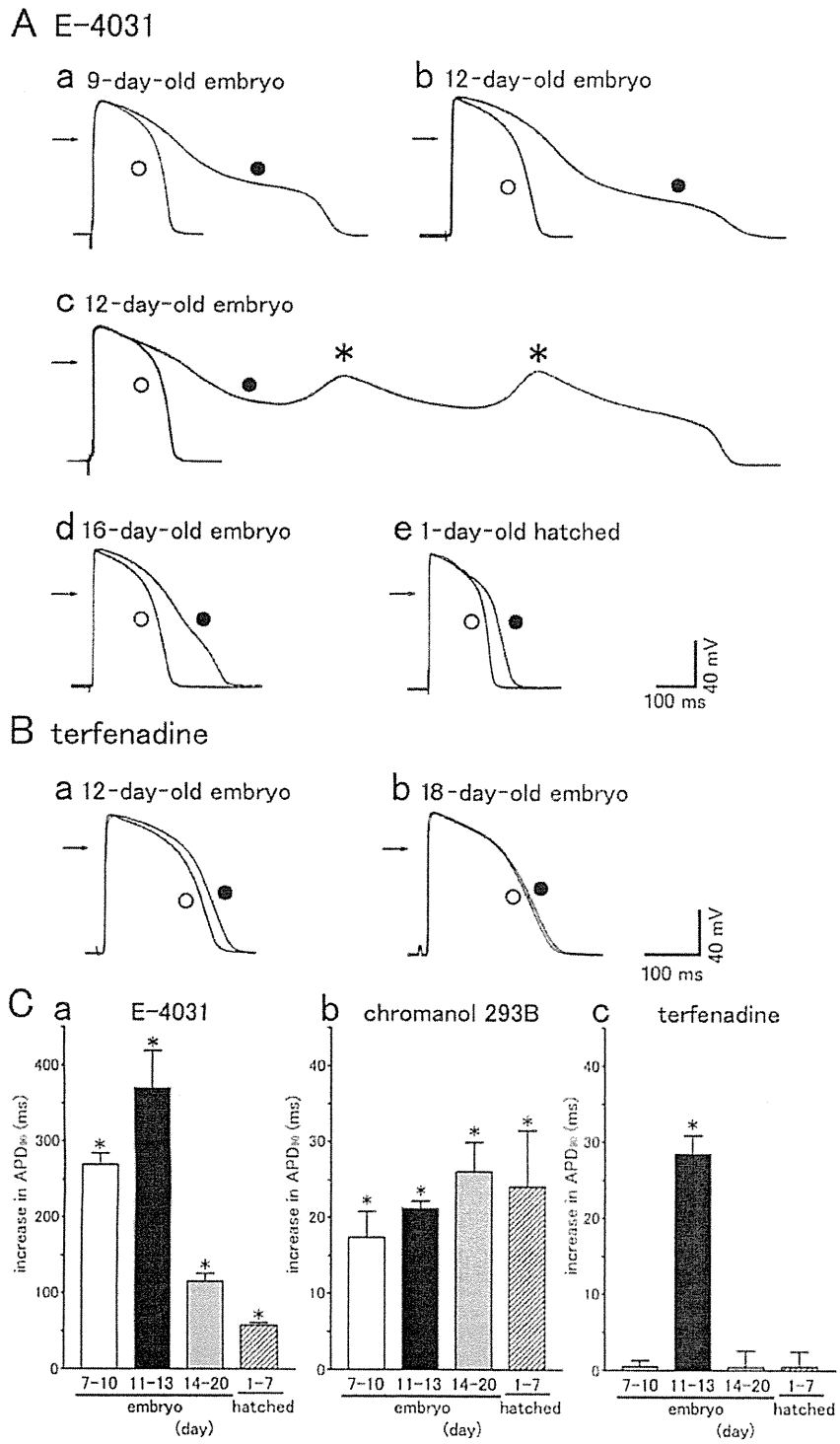

Fig. 1. Effect of K^+-channel blockers on the action potential of isolated chick ventricular myocardium. A: Typical action potential recordings before (open circles) and after (closed circles) the addition of E-4031 (1 μM) in the 9-day-old embryo (a), 12-day-old embryo (b, c), 16-day-old embryo (d), and 1-day-old hatched chick (e). Note that E-4031 induced early after-depolarizations in the 12-day-old embryo (c). B: Typical action potential recordings before (open circles) and after (closed circles) the addition of terfenadine (30 μM) in the 12-day-old embryo (a) and in the 18-day-old embryo (b). Horizontal arrows indicate zero-mV level. Voltage and time calibrations apply to all panels. C: Summarized results for the prolongation of the action potential duration at 90% repolarization (APD_{90}) by 1 μM E-4031 (a), 30 μM chromanol 293B (b), and 30 μM terfenadine (c) in the 7 – 10-day-old embryo (open columns), 11 – 13-day-old embryo (closed columns), 14 – 20-day-old embryo (gray columns), and 1 – 7-day-old hatched chick (hatched columns). Columns and vertical bars are the mean ± S.E.M. from 5 to 6 experiments. Asterisks indicate that the prolongation was statistically significant. Note the difference in the scale of the ordinate.

action potential duration in isolated ventricular tissue from mammals even at 20 μM (15,16). Such presence of "false positive" drugs complicate drug evaluation through action potential duration in tissue preparations (17).

Terfenadine did not prolong action potential duration in the 14 – 20-day-old embryo, which was the same as in isolated mammalian myocardial tissue. However, terfenadine prolonged the action potential duration in the 11 – 13-day-old embryo (Fig. 1: B, Cc). Thus, the 11 – 13-day-old chick embryonic myocardium may be a sensitive model to detect the proarrhythmic activity of drugs. Details such as the density of depolarizing and repolarizing membrane currents and the molecular structure of the delayed rectifier potassium channel in the chick ventricle await further investigation.

In conclusion, we found that the chick ventricle changes its repolarization reserve during development, which provides an interesting model for further studies on myocardial repolarization mechanisms and drug evaluation.

Acknowledgments

This study was supported in part by a Grant-in-Aid from the Ministry of Education, Culture, Sports, Science, and Technology of Japan (#21590293, #21590602, and #22790262) and the Science Research Promotion Fund from the Promotion and Mutual Aid Corporation for Private Schools of Japan. This study was performed in part as "Research on the molecular mechanisms of appearance of age-related diseases by failure of cell function control system, and their prevention and treatment" by the "Research Center for Aging and Age-related Diseases" established in the Toho University Faculty of Pharmaceutical Sciences.

References

1 Sperelakis N, Shigenobu K. Changes in membrane properties of chick embryonic hearts during development. J Gen Physiol. 1972;60:430–453.

2 Satoh H, Sada H, Tohse N, Shigenobu K. [Developmental aspects of electrophysiology in cardiac muscle]. Folia Pharmacol Jpn (Nippon Yakurigaku Zasshi). 1996;107:213–223. (text in Japanese with English abstract)

3 Nouchi H, Tanaka H, Shigenobu K. Pharmacological properties of the developing chick myocardium. Trends Comparative Biochem Physiol. 2005;11:37–45.

4 Tanaka H, Namekata I, Nouchi H, Shigenobu K, Kawanishi T, Takahara A. New aspects for the treatment of cardiac diseases based on the diversity of functional controls on cardiac muscles: diversity in the excitation-contraction mechanisms of the heart. J Pharmacol Sci. 2009;109:327–333.

5 Nouchi H, Kaeriyama S, Muramatsu A, Sato M, Hirose K, Shimizu N, et al. Muscarinic receptor subtypes mediating positive and negative inotropy in the developing chick ventricle. J Pharmacol Sci. 2007;103:75–82.

6 Tanaka H, Komikado C, Namekata I, Nakamura H, Suzuki M, Tsuneoka Y, et al. Species difference in the contribution of T-type calcium current to cardiac pacemaking as revealed by *R*(−)-efonidipine. J Pharmacol Sci. 2008;107:99–102.

7 Namekata I, Tsuneoka Y, Takahara A, Shimada H, Sugimoto T, Takeda K, et al. Involvement of the Na^+/Ca^{2+} exchanger in the automaticity of guinea-pig pulmonary vein myocardium as revealed by SEA0400. J Pharmacol Sci. 2009;110:111–116.

8 Kasuya Y, Matsuki N, Shigenobu K. Changes in sensitivity to anoxia of the cardiac action potential plateau during chick embryonic development. Dev Biol. 1977;58:124–133.

9 Agata N, Tanaka H, Shigenobu K. Developmental changes in action potential properties of the guinea-pig myocardium. Acta Physiol Scand. 1993;149:331–337.

10 Kato Y, Masumiya H, Agata N, Tanaka H, Shigenobu K. Developmental changes in action potential and membrane currents in fetal, neonatal and adult guinea-pig ventricular myocytes. J Mol Cell Cardiol. 1996;28:1515–1522.

11 Sugiyama A. Sensitive and reliable proarrhythmia *in vivo* animal models for predicting drug-induced torsades de pointes in patients with remodeled hearts. Br J Pharmacol. 2008;154:1528–1537.

12 Matsuda T, Takeda K, Ito M, Yamagishi R, Tamura M, Nakamura H, et al. Atria selective prolongation by NIP-142, an antiarrhythmic agent, of refractory period and action potential duration in guinea pig myocardium. J Pharmacol Sci. 2005;98:33–40.

13 Nakaya H, Hashimoto K. QT PRODACT: database construction for the evaluation of the risk of QT interval prolongation by drugs in Japan. J Pharmacol Sci. 2005;99:421.

14 Tanaka H, Nishimaru K, Sekine T, Shijuku T, Shigenobu K. Effects of terfenadine, betotastine and ketotifene on the action potential and membrane currents in isolated guinea-pig myocardium. Res Commun Pharmacol Toxicol. 1997;2:163–174.

15 Masumiya H, Saito M, Ito M, Matsuda T, Noguchi K, Iida-Tanaka N, et al. Lack of action potential-prolonging effect of terfenadine on rabbit myocardial tissue preparations. Biol Pharm Bull. 2004;27:131–135.

16 Tanaka H, Masumiya H, Kato Y, Shigenobu K. Inhibitory effects of terfenadine on the rising phase of action potentials in isolated guinea-pig myocardium. Gen Pharmacol. 1996;27:337–340.

17 Kii Y, Hayashi S, Tabo M, Shimosato T, Fukuda H, Itoh T, et al. QT PRODACT: evaluation of the potential of compounds to cause QT interval prolongation by action potential assays using guinea-pig papillary muscles. J Pharmacol Sci. 2005;99:449–457.

Blocking Effect of NIP-142 on the KCNQ1/KCNE1 Channel Current Expressed in HEK293 Cells

Iyuki NAMEKATA,[a] Noriko TSURUOKA,[a] Yayoi TSUNEOKA,[a] Tomoyuki MATSUDA,[a,b] Akira TAKAHARA,[a] Yoshio TANAKA,[a,c] Takeshi SUZUKI,[a,d] Tetsuo TAKAHASHI,[e] Naoko IIDA-TANAKA,[a,f] and Hikaru TANAKA*,[a]

[a] *Department of Pharmacology, Faculty of Pharmaceutical Sciences, Toho University;* [c] *Department of Chemical Pharmacology, Faculty of Pharmaceutical Sciences, Toho University;* [e] *Department of Biophysical Chemistry, Faculty of Pharmaceutical Sciences, Toho University; Funabashi, Chiba 274–8510, Japan:* [b] *Biological Research Laboratories, Nissan Chemical Industries, Ltd.; Shiraoka, Saitama 349–0294, Japan:* [d] *School of Material Science, Japan Advanced Institute of Science and Technology; Tatsunokuchi, Ishikawa 923–1292, Japan: and* [f] *Department of Food Science, Otsuma Women's University; Chiyoda-ku, Tokyo 102–8357, Japan.*

Received September 14, 2010; accepted October 29, 2010; published online November 5, 2010

We examined the effect of NIP-142, a benzopyran compound with terminating effect on experimental atrial arrhythmia, on the KCNQ1/KCNE1 channel, which underlies the slow component of the cardiac delayed rectifier potassium channel (I_{Ks}). NIP-142, as well as chromanol 293B, showed concentration-dependent blockade of the current expressed in HEK293 cells; the EC_{50} value of NIP-142 and chromanol 293B for the inhibition of tail current was 13.2 μM and 4.9 μM, respectively. These results indicate that NIP-142 has blocking effect on the KCNQ1/KCNE1 channel current.

Key words NIP-142; KCNQ1; KCNE1; atrial fibrillation

Atrial fibrillation is one of the most frequent types of arrhythmia in clinical practice. It is reported to double the risk of deaths due to cardiovascular diseases and to be the major risk factor for thromboembolism, especially cerebral embolism.[1] At present, atrial fibrillation is mainly treated with class I antiarrhythmic agents such as pilsicainide and flecainide, or class III antiarrhythmic agents such as dofetilide and amiodarone,[2—4] but the major problem with these agents is that they also affect ventricular excitation and repolarization. Thus, drugs with atrial selectivity are desired for the treatment of atrial fibrillation.

NIP-142, (3*R**,4*S**)-4-cyclopropylamino-3,4-dihydro-2,2-dimethyl-6-(4-methoxyphenylacethylamino)-7-nitro-2*H*-1-benzopyran-3-ol, is a benzopyran derivative with terminating effects on canine vagal stimulation-induced atrial fibrillation model and on canine Y-shaped incision-induced atrial flutter model.[5—7] These effects have been attributed to prolongation of atrial refractory period. The prolongation of the refractory period and action potential duration (APD) by NIP-142 was observed in the atrium,[5,8] but not in the ventricle.[8] This may indicate that NIP-142 is less likely to disturb ventricular repolarization when applied for the treatment of atrial arrhythmia.

Concerning the molecular mechanisms for the action potential prolongation by NIP-142, blocking effects on potassium currents such as the acetylcholine-activated potassium current (I_{KACh})[8,9] and the ultrarapid component of the delayed rectifier potassium current (I_{Kur})[10] has been reported. The blocking effect on the rapid component of the delayed rectifier potassium current (I_{Kr}) was observed only at higher concentrations. The fast component (I_{Kr}) and the slow component (I_{Ks}) of the delayed rectifier potassium current are the two major currents responsible for atrial repolarization in species including the guinea-pig and human.[11] However, the effect of NIP-142 on I_{Ks} has not yet been reported. In the present study, we examined the effect of NIP-142 on currents through expressed potassium channel subunits KCNQ1/KCNE1, which underlie I_{Ks}.

MATERIALS AND METHODS

Preparation of HEK293 Cells Expressing Human KCNQ1/KCNE1 Channel Currents cDNA fragments for human KCNQ1 and KCNE1, which encode the two subunits of the I_{Ks} channel, were amplified by polymerase chain reaction from a human heart cDNA library (Takara Shuzo Co., Ltd., Kyoto, Japan) with oligonucleotide primers designed based on the published mouse cDNA sequence of KCNQ1 (GenBank accession number U89364) and KCNE1 (GenBank accession number NM000219), and assembled to obtain the full length cDNAs. They were inserted into the vector pIRES (Clontech, Palo Alto, CA, U.S.A.) to yield a tricistronic expression vector from which a single mRNA coding KCNQ1, KCNE1, and the neomycin resistance protein is transcribed. This vector, together with the vector pIRES-hrGFP-1α (Stratagene, Garden Grove, CA, U.S.A.), which encodes the green fluorescence protein (GFP), was introduced into HEK293 cells with lipofectamine (Invitrogen, Tokyo) and stable transformants were obtained by clone culture in the presence of G418 (500 μg/ml), a neomycin analog. Stable transformants of HEK293 cells expressing KCNQ1/KCNE1 channels were obtained as described in our previous report.[9] The cells expressing either channel were plated on glass coverslips 48 to 72 h before electrophysiological experiments.

Electrophysiological Recording of Expressed KCNQ1/KCNE1 Channel Current Whole-cell voltage clamp experiments were performed with HEK293 cells expressing KCNQ1/KCNE1 channels in a chamber mounted on the stage of an inverted microscope. The chamber was perfused continuously at a flow rate of 1.0 to 2.0 ml/min and the temperature was maintained at 22—25 °C. The external solution

* To whom correspondence should be addressed. e-mail: htanaka@phar.toho-u.ac.jp

was of the following composition: 128.0 mM NaCl, 20.0 mM KCl, 1.8 mM $CaCl_2$, 1 mM $MgCl_2$, 0.33 mM NaH_2PO_4, 5.0 mM *N*-(2-hydroxyethyl)piperazine-*N'*-2-ethanesulfonic acid (HEPES), 10.0 mM glucose (pH 7.4 with NaOH). The patch pipette solution was of the following composition: 100 mM KOH, 40 mM KCl, 70 mM aspartic acid, 1 mM $MgCl_2$, 5 mM ATP-K_2, 5 mM creatine phosphate-K_2, 5 mM HEPES, 10 mM ethylene glycol bis(2-aminoethylether)-*N,N,N',N'*-tetraacetic acid (EGTA) (pH 7.2 with KOH). Pipette tip resistances were 2 to 4 MΩ when filled with the patch pipette solution. The KCNQ1/KCNE1 channel current was measured as the amplitude of the peak tail current on return to a holding potential of −40 mV from 3 s voltage clamp pulses. Data acquisition and analyses were performed with the system described previously[9] including a patch-clamp amplifier (Axopatch 1D; Axon Instruments, Foster City, CA, U.S.A.), a personal computer (Prolinea 486; Compaq, Houston, TX, U.S.A.) and pCLAMP software (Axon).

Drugs and Chemicals NIP-142 was synthesized and provided by Nissan Chemical Industries (Tokyo, Japan). NIP-142 was added to the bath solution from a stock solution (100 mM) in 0.1 M HCl. The final concentration of HCl in the measuring bath (<0.1 mM) did not affect any of the experimental parameters measured. All other chemicals were commercial products of the highest available grade of quality.

RESULTS

In whole cell voltage clamped HEK293 cells expressing the KCNQ1/KCNE1 channel, depolarization to membrane potentials more positive than −10 mV induced voltage- and time-dependent outward currents. On repolarization to −40 mV, outward tail currents were observed (Figs. 1A, C). The peak amplitude of the tail current after a depolarizing pulse to 20 mV was 8.6±0.8 pA/pF (n=10).

Chromanol 293B, at 1 to 30 μM, concentration-dependently reduced the outward currents on depolarization and the tail currents on repolarization (Figs. 1A, B). The current density of the tail current after a depolarizing pulse to 20 mV in the absence and presence of 1, 3, 10 and 30 μM chromanol 293B was 7.5±1.4 pA/pF (n=10), 5.4±0.4 pA/pF (n=4), 4.5±0.9 pA/pF (n=5), 2.2±0.2 pA/pF (n=6) and 0.1±0.2 pA/pF (n=4), respectively. The EC_{50} value for the inhibition of tail current on repolarization from 20 mV was 4.9 μM (Fig. 1E).

NIP-142, at 10 and 30 μM, concentration-dependently reduced the outward currents on depolarization and the tail current on repolarization (Fig. 1C). The current density of the tail current after a depolarizing pulse to 20 mV in the absence and presence of 1, 10 and 30 μM NIP-142 was 9.7±0.7 pA/pF (n=10), 9.5±1.4 pA/pF (n=4), 5.4±1.0 pA/pF (n=5) and 1.8±0.5 pA/pF (n=5), respectively. The EC_{50} value for the inhibition of tail current on repolarization from 20 mV was 13.2 μM (Fig. 1E).

DISCUSSION

NIP-142 concentration-dependently blocked the KCNQ1/KCNE1 channel current with an EC_{50} value of 13.2 μM (Fig. 1). The reported EC_{50} value of NIP-142 for the GIRK1/4 channel current is 0.64 μM,[9] that for the Kv1.5

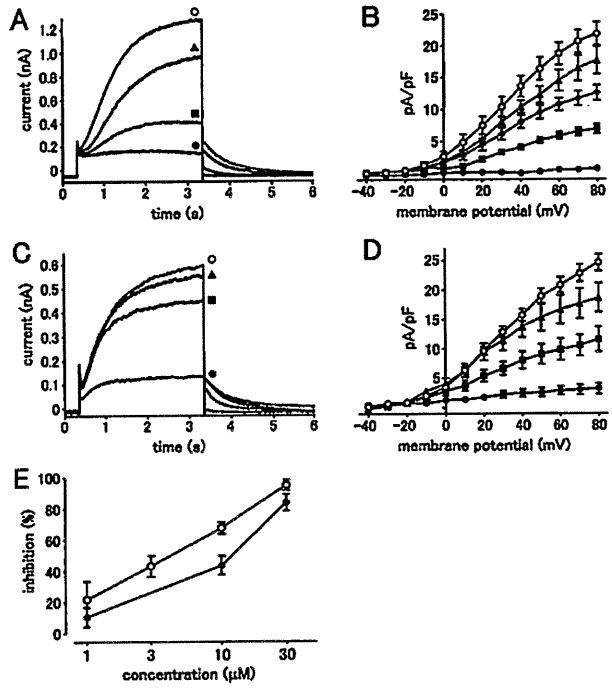

Fig. 1. Effect of Chromanol 293B and NIP-142 on KCNQ1/KCNE1 Channel Currents Expressed in HEK293 Cells

(A) Typical recordings in the absence (open circles) and presence of 1 μM (closed triangles), 10 μM (closed squares) and 30 μM (closed circles) chromanol 293B. (B) Summarized current–voltage relationships for the peak outward tail current on repolarization to −40 mV from a 3 s depolarization to various test potentials in the absence (open circles) and presence of 1 μM (closed triangles), 3 μM (closed diamonds), 10 μM (closed squares) and 30 μM (closed circles) chromanol 293B. (C) Typical recordings of the effects of NIP-142. (D) Summarized current–voltage relationships for the peak outward tail current on repolarization to −40 mV from a 3 s depolarization to various test potentials in the absence (open circles) and presence of 1 μM (closed triangles), 10 μM (closed squares) and 30 μM (closed circles) NIP-142. (E) Concentration–response relationship for blockade by chromanol 293B (open circles) and NIP-142 (closed circles) of the peak tail current on repolarization from 20 mV. Symbols and bars represent the mean±S.E.M from 4 to 8 experiments.

channel current is 4.8 μM,[10] and that for the HERG channel current is 44 μM.[9] The blocking potency of NIP-142 on the KCNQ1/KCNE1 channel current was relatively low, suggesting that the prolongation of atrial action potential by the compound is mainly produced by blockade of potassium currents other than I_{Ks}, especially the acetylcholine-activated potassium current. However, as the concentration range of NIP-142 (10 to 100 μM) to prolong the atrial action potential[8] overlaps that to inhibit the KCNQ1/KCNE1 channel current (Fig. 1E), the possibility that I_{Ks} blockade contributes to the effect of NIP-142 can not be totally excluded. The I_{Ks} current is known to be increased by factors such as β-adrenergic stimulation[12] or angiotensin II.[13] A gain-of-function mutation of KCNQ1 was reported to cause atrial fibrillation.[14] Development of novel I_{Ks} blockers with antiarrhythmic activity are in progress.[15] Thus, the I_{Ks}-blocking effect of NIP-142 may contribute to its antifibrillatory activity under certain pathological conditions.

NIP-142 was reported not to prolong the action potential duration in isolated guinea-pig ventricular tissue preparations,[8] despite its inhibitory effect on the KCNQ1/KCNE1 channel current. One explanation for this apparent discrepancy is the variation in sensitivity among experimental sys-

tems. There are cases in which potency of ion channel inhibitors are higher in voltage-clamped single cells than in myocardial tissue preparations (*S*(+)-Efonidipine[16]). The extent of I_{Ks}-blockade by NIP-142 in tissue preparations might be smaller than expected from the present results. Another possible explanation for the lack of action potential prolongation by NIP-142 in the ventricle is its blocking effect on calcium channels. We have observed that NIP-142 has blocking effect on the L-type calcium channel,[17] which may counteract its action potential-prolonging effect through potassium channel blockade. In any case, the details for the mechanisms of action of NIP-142 remain to be investigated.

Acknowledgments This study was supported in part by the Science Research Promotion Fund from the Promotion and Mutual Aid Corporation for Private Schools of Japan (for Y. Tanaka and H. Tanaka). This study was partly performed as a part of the project "Research on the molecular mechanisms of appearance of age-related diseases by failure of cell function control system, and their prevention and treatment" by the "Research Center for Aging and Age-Related Diseases" established in the Toho University Faculty of Pharmaceutical Sciences.

REFERENCES

1) Sugimoto T., Hayakawa K., Kasanuki H., "Atrial Fibrillation, Flutter, and Tachycardia," ed. by Hayakawa K., Kasanuki H., Igaku-Shoin, Tokyo, 1999, pp. 14—18.
2) Aliot E., Denjoy I., *Am. J. Cardiol.*, **77**, 66A—71A (1996).
3) Iwasaki H., Takahara A., Nakamura Y., Satoh Y., Nagai T., Shinkai N., Sugiyama A., *J. Pharmacol. Sci.*, **110**, 410—414 (2009).
4) Lenz T., Hilleman D., *Drugs Today* (Barc), **36**, 759—771 (2000).
5) Nagasawa H., Fujiki A., Fujikura N., Matsuda T., Yamashita T., Inoue H., *Circ. J.*, **66**, 185—191 (2002).
6) Tanaka H., Hashimoto N., *Cardiovas. Drug Rev.*, **25**, 342—356 (2007).
7) Hashimoto N., Tanaka H., "Progress in Cardiac Arrhythmia Research," ed. by Tarkowicz I. R., Nova Science Publishers, Hauppague, 2009, pp. 125—139.
8) Matsuda T., Takeda K., Ito M., Yamagishi R., Tamura M., Nakamura H., Tsuruoka N., Saito T., Masumiya H., Suzuki T., Iida-Tanaka N., Itokawa M., Yamashita T., Tsuruzoe N., Tanaka H., Shigenobu K., *J. Pharmacol. Sci.*, **98**, 33—40 (2005).
9) Matsuda T., Ito M., Ishimaru S., Tsuruoka N., Saito T., Iida-Tanaka N., Hashimoto N., Yamashita T., Tsuruzoe N., Tanaka H., Shigenobu K., *J. Pharmacol. Sci.*, **101**, 303—310 (2006).
10) Matsuda T., Masumiya H., Tanaka N., Yamashita T., Tsuruzoe N., Tanaka Y., Tanaka H., Shigenobu K., *Life Sci.*, **68**, 2017—2024 (2001).
11) Bosch R. F., Gaspo R., Busch A. E., Lang H. J., Li G. R., Nattel S., *Cardiovas. Res.*, **38**, 441—450 (1998).
12) Sanguinetti M. C., Jurkiewicz N. K., Scott A., Siegl K. S., *Circ. Res.*, **68**, 77—84 (1991).
13) Zankov D. P., Omatsu-Kanbe M., Isono T., Toyoda F., Ding W. G., Matsuura H., Horie M., *Circulation*, **113**, 1278—1286 (2006).
14) Chen Y. H., Xu S. J., Bendahhou S., Wang Y., Xu W. Y., Jin H. W., Sun H., Su X. Y., Zhuang Q. N., Yang Y. Q., Li Y. B., Liu Y., Xu H. J., Li X. F., Ma N., Mou C. P., Chen Z., Barhanin J., Huang W., *Science*, **299**, 251—254 (2003).
15) Salataa J. J., Scinickb H. G., Lynch J. J. Jr., *Curr. Med. Chem.*, **11**, 29—44 (2004).
16) Tanaka H., Namekata I., Ogawa T., Tsuneoka Y., Komikado C., Takahara A., Iida-Tanaka N., Izumi-Nakaseko H., Tsuru H., Adachi-Akahane S., *Eur. J. Pharmacol.*, **649**, 263—267 (2010).
17) Matsuda T., Masumiya H., Saito T., Tanaka H., Shigenobu K., *Jpn. J. Pharmacol.*, **79** (Suppl. I), 178P (1999).